A

Dissertation Report

On

Development and Experimental Investigation on Nano-Fluid Based I.C. Engine Coolant

Submitted in Partial Fulfillment for the Award of

Master of Technology in Energy Engineering

By

SAURABH KUMAR

2013PME5133

Under the Guidance of

Dr. S.L. Soni

Professor

Department of Mechanical Engineering

MNIT, Jaipur

DEPARTMENT OF MECHANICAL ENGINEERING

MALAVIYA NATIONAL INSTITUTE OF TECHNOLOGY, JAIPUR

JUNE 2015

DEPARTMENT OF MECHANICAL ENGINEERING
MALAVIYA NATIONAL INSTITUTE OF TECHNOLOGY
JAIPUR (RAJASTHAN)-302017

CERTIFICATE

This is certified that the dissertation report entitled **"Development and Experimental Investigation on Nano-Fluid Based I.C. Engine Coolant"** prepared by **Saurabh Kumar** (ID-2013PME5133), in the partial fulfillment of the award of the Degree **Master of Technology** in **Energy Engineering** of Malaviya National Institute of Technology Jaipur is a record of bonafide research work carried out by him under my supervision and is hereby approved for submission. The contents of this dissertation work, in full or in parts, have not been submitted to any other Institute or University for the award of any degree or diploma.

Date:

Place:

Dr. S.L. Soni

Professor

Department of Mechanical Engineering

MNIT, Jaipur

DEPARTMENT OF MECHANICAL ENGINEERING
MALAVIYA NATIONAL INSTITUTE OF TECHNOLOGY
JAIPUR (RAJASTHAN)-302017

DECLARATION

I **Saurabh Kumar** hereby declare that the dissertation entitled **"Development and Experimental Investigation on Nano-Fluid Based I.C. Engine Coolant"** being submitted by me in partial fulfillment of the degree of **M. Tech. (Energy Engineering)** is a research work carried out by me under the supervision of **Prof. S. L. Soni,** and the contents of this dissertation work, in full or in parts, have not been submitted to any other Institute or University for the award of any degree or diploma. I also certify that no part of this dissertation work has been copied or borrowed from anyone else. In case any type of plagiarism is found out, I will be solely and completely responsible for it.

Date: Saurabh Kumar

M.Tech. (Energy Engg.)

Place: 2013PME5133

ACKNOWLEDGEMENT

I feel immense pleasure in conveying my heartiest thanks and profound gratitude to my supervisor **Dr. S.L. Soni**, Professor, Department of Mechanical Engineering for providing me with his generous guidance, valuable help and endless encouragement by taking personal interest and attention. No words can fully convey my feelings of respect and regards for him.

I want to express my deepest gratitude to **Prof. Dilip Sharma, Dr. G.D. Aggarwal, Prof. Jyotirmay Mathur and Dr. Nirupam Rhotagi** for showing me the right direction during the duration of this project. I also express my gratitude to **Prof. G.S. Dangayach** (HOD) Mechanical Engineering Department for providing valuable suggestions and words of encouragement.

I am indebted to Mr. R.C Meena, Mr. Kolahal, Mr. Mahaveer Singh staff members of I.C. engines laboratory and to my colleagues Mr. Vikas Mahala, Mr. Ranaveer Pratap Singh and Mr. Pushkar Chandra, for helping me throughout my dissertation work.

I would like to pay high regards to my **Parents** for their sincere inspiration and motivation throughout my dissertation work and lifting me uphill this phase of life. Lastly, but not least I thank one and all who have helped me directly or indirectly in completion of the report.

(Saurabh Kumar)

ABSTRACT

The aim of the present study is to investigate the performance of Al_2O_3-Water nano-fluid based engine coolant. Nano-fluid based I.C. Engine coolant gives better thermal performance as compared to conventional coolant when used in engine radiator. The I.C. Engine radiator is based on the principle of cross flow heat exchanger transferring heat to different working fluids (coolant to ambient air in this case). Heat is directly absorbed by the fluid flowing through the water jacket.

This technique of directly absorbing the excess heat seems to be of great importance as it results in better operating temperature control for efficient combustion environment. In a liquid cooled engine heat is transferred to the radiator tubes and finally to ambient air, this leads to optimum temperature control and better cooling characteristics in comparison to air cooling.

For experimental study firstly experimental sonication time determination and stability analysis was done for two most commonly used nano-fluids i.e. Titanium Dioxide and Aluminum Oxide based nano-fluids. Sonication time is the duration for which the nanofluid mixture is to be agitated to obtain a stable colloidal mixture. Stability analysis included the time for which the prepared sample remains in colloidal form and nanoparticles do not settle at the bottom. Thermal conductivity approach was used in the above analysis. Experimental Setup was prepared with the available radiator of 900 cm^2 area (width 30 cm and length 30 cm). Setup was installed on the single cylinder water cooled I.C. Engine in I.C. Engine lab of Mechanical Engineering Department MNIT, Jaipur. The radiator has 104 vertical pass tubes with horizontal fins to prevent “in tube” particle deposition. The flow rate was measured by using pitot tube method.

Water and Al_2O_3-Water nano-fluid was selected as working fluid due to its superior heat transfer properties. Nano-fluid was used as working fluid as it has better thermal properties. Nanoparticle Al_2O_3 with average particle size 30 nm was used (refer to Appendix 2). Various weight fractions (0.2%, 0.4%, 0.6%, 0.8% and 1.0%) were used during experimentation. Nano-fluid was prepared using two step method.

The experimental study was divided in two phases, in first phase experiments were conducted on two different nanoparticles (Al_2O_3 and TiO_2) for determination of sonication time and stability. In second phase selected nanofluid was used as engine coolant at constant flow rate (15 lpm) and weight fraction of Nano-fluid was changed from 0.2% to 1.0%. Same procedure was followed for different loads and the performance of radiator was analyzed. Time to cool-down was also analyzed by running the engine at full load for 10 min (after experimentation) and then idled till the temperature drops to initial values.

The performance with nano-fluid based coolant was better than the only water/coolant as working fluid. The performance of 1.0 % nano-fluid was best among the five concentrations which were used during experiment for all load conditions. For low weight fraction thermal conductivity was less and for higher volume fraction thermal conductivity was increased but the problem of stability and agglomeration occurred. The engine vibrations were utilized to prevent any particle deposition during engine run time and to re-mix the deposited particles during next engine run.

Thermal performance of nano-fluid was analyzed for each weight fraction of nanofluid for different loads (0 kW to 3.5 kW) and it was observed that for low weight fraction of nanofluid the performance is similar to conventional coolant at all loads.

At higher weight fraction (0.6%, 0.8%, 1.0%) the best thermal performance was given by 1.0%. As the thermal conductivity is higher for high weight fraction, it takes less time to absorb heat from water jacket. Heat rejections are higher for higher weight fractions for a given flow rate.

Percentage frontal area reduction was calculated from the coolant heat rejection data obtained from the experiment. The area reduction was found to be directly proportional to the heat rejection from the radiator.

TABLE OF CONTENTS

TABLE OF CONTENTS

LIST OF FIGURES

LIST OF TABLES

NOMENCLATURE

$\dot{m}$	Mass flow rate (kg/s)
C_p	Specific heat (kJ/kg K)
C_{pc}	Coolant Specific heat (kJ/kg K)
H	Heat (W)
T_o	Outlet Temperature (℃)
T_i	Inlet Temperature (℃)
T_c	Coolant temperature (℃)
T_a	Ambient air temperature (℃)
T_g	Exhaust gas temperature (℃)
ΔT	Outlet inlet temperature difference (℃)
A	frontal area (m^2)
ϕ	Volume Fraction
k	Thermal conductivity (W/m K)
ρ	Density (kg/m^3)
p.f	Power factor
e.m.f	Electromotive force
EG	Ethylene Glycol

Abbreviations

UC	Ultrasonic Cleaner
lpm	Liter per Minute
nm	Nanometer
ppm	Parts per Million
ASHRAE	American Society of Heating, Refrigeration and Air-conditioning Engineers
BIS	Bureau of Indian Standards
CPVC	Chlorinated Poly-Vinyl Chloride
HTF	Heat Transfer Fluid
wf.	Weight fraction
vf.	Volume fraction
H-C	Hamilton- Crossier

Subscripts

eff	Effective
L	Loss
p	Particle
f	Fluid
U	Useful
i	Inlet
o	Outlet
a	Ambient
g	Gas
c	Coolant

Chapter 1 Introduction

I.C. Engine cooling is always been a challenge to achieve. The metallurgical constrains restricts the maximum operating temperature for internal combustion engines. The materials used in these engines are mainly cast iron, aluminum and steels which have upper temperature limit of 600 to 700°C. This calls for mean engine temperature to be in the range of 150 to 250 °C. The maximum cycle temperature is about 2100 °C. The heat dissipation to cylinder walls by convection and radiation brings the average temperature in the above mentioned range.

The I.C. Engine cooling is done by two methods namely direct (air cooling) and indirect (water/liquid cooling). In former type cylinder block has fins attached which dissipate the heat from the cylinder walls to ambient air. A forced circulation fan is often used on larger engines. In liquid cooled engines a water jacket is provided between cylinder and cylinder block. A liquid to air heat exchanger (called radiator) is used to dissipate the excess heat to ambient air. The liquid cooling results in overall smaller engine dimensions and better temperature control.

1.1 Liquid cooling circuit

The cooling circuit of engine consists of water jacket in cylinder block, radiator, connecting hoses, fluid circulating fan and thermostatic valve. As the engine starts the cylinder walls begins to heat up. The coolant present in water jacket absorbs the heat and this raises its temperature. A recirculation pump driven by the crankshaft transports this hot water/coolant to the radiator through the hoses. The radiator has small parallel metallic tubes through which coolant flows thereby exchanging heat with thin fins attached to the tubes. The attached fins eventually reject absorbed heat to the environment. A fan is used on air side to ensure forced flow conditions. Sometime a thermostatic valve is used to stop the coolant flow during initial minutes to sufficiently warm up the engine for efficient operation.

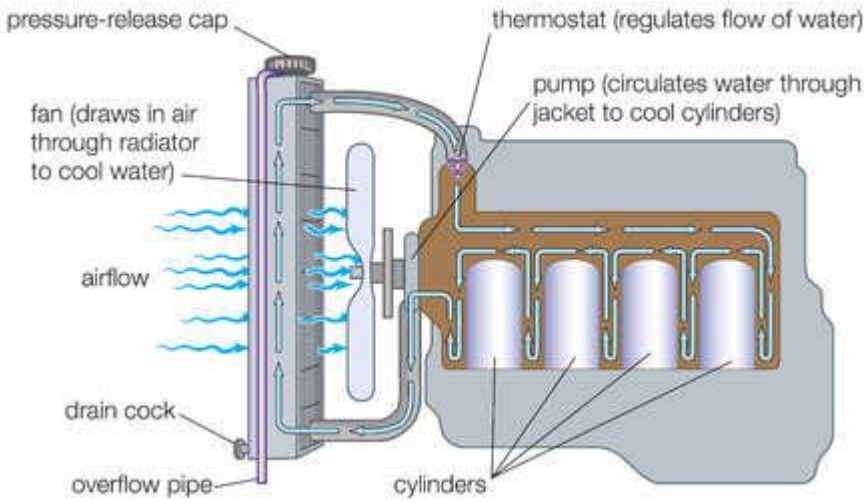

Figure 1 Schematic diagram of liquid cooling circuit of I.C. Engine

The diagram above shows the basic components of a liquid cooled engine. In natural circulation mode the direction of coolant flow will be downwards through the radiator as cold fluid is heavier due to greater density. In case of forced circulation the flow direction can be either side. Even the horizontal flow radiators are used in some force circulation engines.

1.1.1 Coolants

Coolant is the working fluid in the cooling circuit on I.C. Engine. It receives thermal energy from the engine cylinder water jacket and transfers it to radiator tubes. In liquid cooled engines following coolants are typically used : water, ethylene glycol, synthetic oils. Water is most widely used coolant in stationary engines primarily due to negligible cost and tremendous availability. In mobile engines as in vehicles, ethylene glycol-water mixture is used as coolant. As vehicles have to travel in variety of climates (sub-zero to more than 50°C) sometimes water cooling is no longer feasible. Ethylene glycol when mixed with water is known to depress the freezing point of water by few degrees depending on concentration and boiling point is also raised above 100°C. This property makes it ideal for vehicular engines.

Other form of liquid cooling in engines is to directly cool the lubricating oil and recirculate it in every part of the engine to carry the generated heat. This type of cooling is

used in very compact engines like Wankel and Duke Engines. Main focus is on water based coolants therefore literature regarding oil cooling is omitted here.

1.1.2 Circulation system

It refers to the system used to circulate the coolant through the cooling circuit. The coolant is expected to take away the heat generated in the cylinder from the cooling jacket and reject that heat to the radiator tubes, from where it is transferred to the ambient air through fins. To ensure the close cycle reusability of the coolant it is repeatedly transported to and from cooling jacket (and radiator). This can either be done through natural circulation (thermo-syphon) due to density difference between hot and cold fluid or by forced circulation by a fluid pump. To meet varied cooling requirements at different loads and speed conditions a flow control valve is installed.

The main components of coolant circulation system are as follows:

- Radiator
- Connecting hoses
- Water jacket
- Recirculation pump
- Radiator fan
- Flow control valve

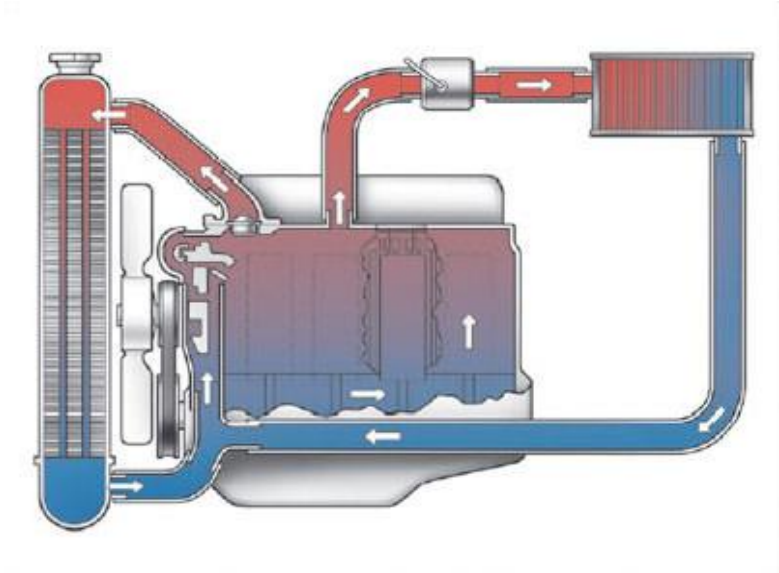

Figure 2-Coolant recirculation system

1.1.3 Automotive Radiator

Radiator is a device used in heat exchange applications to transfer heat from one fluid medium to another. In construction and working it is not different than any other heat exchanger. The main constructional features of automotive radiator are as follows:

- Inlet hose and reservoir
- Coolant carrying metallic tubes
- Outlet hose and reservoir
- Overflow valve
- Pressure release valve

Radiators are installed in such locations where they exposed to maximum ambient air for maximum efficiency. Parallel tube radiators are most commonly used automotive radiators because of simplistic design, less initial and maintenance cost, long life and simple working. Smaller engines use thermo syphon (natural circulation) system but bigger and high rated engines have to use forced circulation pump. The flow rate through the cooling circuit can be varied either manually or by thermostatic valve.

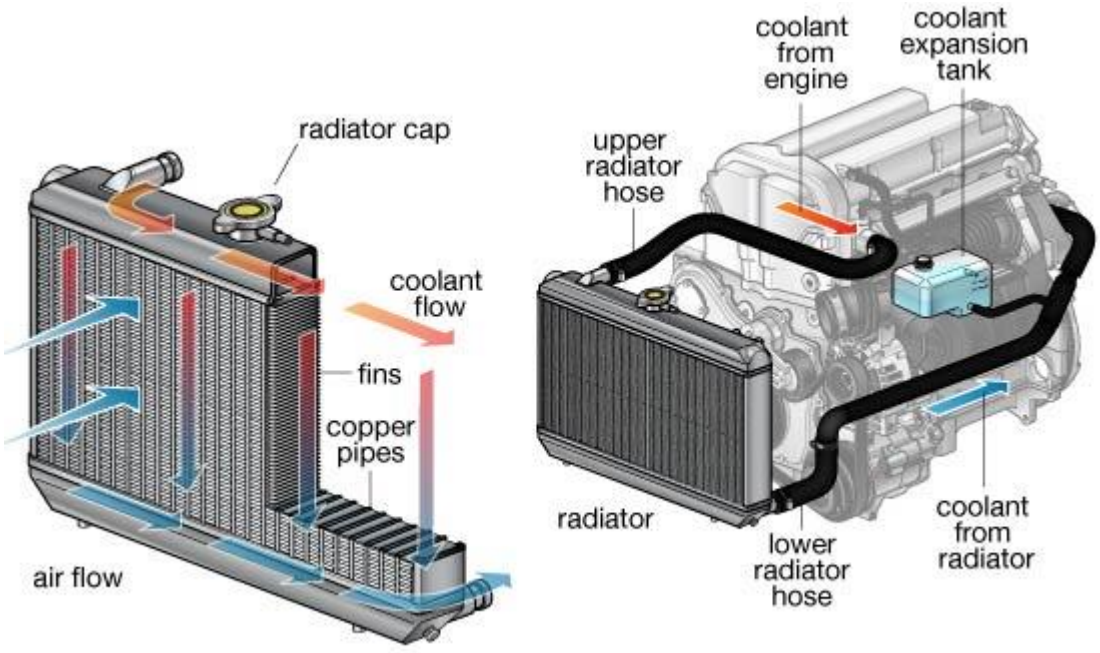

Figure 3-Typical automotive radiator

The automotive radiator can be in vertical tube or horizontal tube arrangement. The vertical tube arrangement allows coolant to flow in downward direction as it cools down. This allows for natural circulation of coolant hence these are typically used for thermo syphon systems. The coolant flows in horizontal direction in horizontal tube arrangement. It requires an external circulation pump for coolant flow. More controlled flow is possible in case of the latter. For sufficiently large stationary engines vertical tube radiators with recirculation pump are used with a fan for radiator air flow.

1.1.4 Connecting hoses

These are synthetic rubber based flexible pipes of suitable diameter and length. These connect the water jacket with radiator and coolant pump and maintain a closed system. The hoses are connected to above mentioned components with the help of hose clamps. The recently developed nylon based hoses are more durable and capable of bearing higher temperatures. The hoses are reinforced by polymer fibers to ensure high pressure and temperature bearing properties.

Figure 4: Connecting hose of radiator

1.1.5 Recirculation pump

It is used in forced circulation systems for recirculating the coolant in the cooling circuit. The pump is a typical centrifugal pump and is generally driven by a belt running through pulley attached to crankshaft. A v-belt is used to drive the pump pulley. The speed of pump depends on the speed of the engine, hence at higher speeds the coolant flow rate is higher and air flow velocity through radiator is also higher. This allows more heat to be taken away from the engine.

In constant speed engines like used in power generation, the engine speed has to be kept constant. In India electricity is generated at 50 Hz, so a 4 pole alternator is required to run at 1500 RPM at all loads. This is achieved by governor controlled fuel flow. In such engines the crank driven pump will have same flow rate at all loads, hence the coolant temperature varies in accordance with load on engine. The jacket coolant outlet temperature varies almost linearly with load.

1.1.6 Radiator Fan

In stationary engines or in automobile at rest there is negligible air flow across the radiator. This may result in overheating of the engine. To avoid this problem an air circulation fan is installed in front of radiator to ensure air flow across the radiator in all conditions. In stationary engines the fan is attached to the coolant pump pulley and it rotates at the pump speed. The belt connecting pump pulley and crank pulley is often called “fan belt”. Modern automotive engines with horizontal radiator tube arrangement have an electric radiator fan. It only works when required i.e. when vehicle is stationary.

Figure 5: Fan attached to radiator

1.1.7 Flow control valve and pressure release valve

These valves are installed in cooling system to ensure safety of the components. Flow control valve is fitted in coolant circuit typically at jacket coolant outlet. This valve opens and flow starts when engine has reached a predefined operating temperature. This ensures a quick engine warm up.

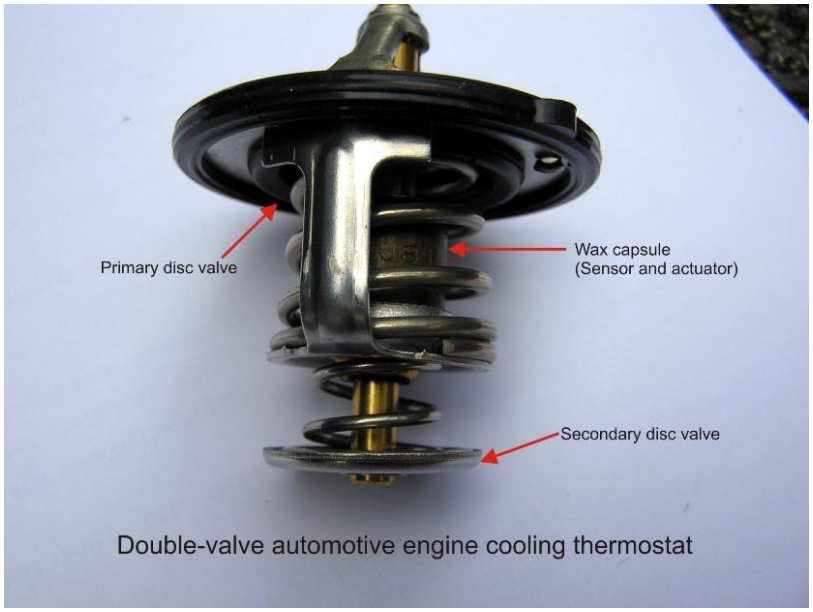

Figure 6: Thermostatic coolant valve

Pressure release valve is typically integrated with radiator cap. When coolant becomes hotter it tends to expand, but is not allowed to do so due to non-flexible components. Therefore the pressure in the system rises which can damage the coolant flow circuit. To release this excess pressure, a pressure actuated release valve opens to allow excess coolant to escape through drain pipe and pressure of the system retain previous values. The operation and principle is similar to pressure cooker.

In order to improve the performance of automotive radiators some kind of improvements in design or optimization in operating parameters are necessary so that overall efficiency can be increased. Parameters which affect the performance of radiator are:

- Working fluid
- Flow rate of fluid
- Ambient air conditions

- Air flow available in front of radiator

1.2 Advantage and limitations of radiator cooling

Advantage

- Better temperature control
- Overall smaller system dimensions
- Easier to monitor the operating temperatures
- Take less time to attain a optimum temperature

Limitations

- Higher initial cost
- More chances of leakage.
- More component wear and tear.

1.3 Need of the study

Because of many limitations of conventional radiator cooling system we have to find an alternative for it to overcome these limitations. Following are the limitations:

- Large frontal area is required for less amount of useful heat rejection.
- The transient temperature response is not instantaneous which results in thermal stresses being build up in various parts of engine.
- High pumping power due to higher coolant flow rate.

These limitations reflect need of alternative methods for the improvement in efficiency. Automotive radiator using nano-fluid seems to have the potential of improving heat transfer characteristics.

In nano-fluid based coolant the transient response is very fast as compared to conventional coolant. Therefore it is considered a feasible alternative in the near future.

1.4 Nano-fluids

It refers to a class of nano-sized metallic and non-metallic particles mixed in a liquid medium as colloidal solutions. The particle size (diameter) usually lies in the range of 5 nm to 150 nm. The metals and their oxides are most widely used in nano-fluid preparation. Some non-metallic materials for nano-fluid preparation are diamond, plastic, and CNT (carbon nanotubes). CNT is found to have superior thermal properties in the entire material catalogue available, but its use usually limited due to higher cost.

Preparation of nanoparticles is usually done by crushing at very low temperatures but the particle size is limited to 100nm. Newer methods like chemical and physical vapor deposition, electrochemical methods results in much smaller particle sizes. The morphology may be spherical, cylindrical or irregular shape. The spherical particles are most commonly found.

1.4.1 Nano-fluid preparation

One step method

The single-step preparation process indicates the synthesis of nano-fluids in one-step. Several single-step methods have been developed for nano-fluid preparation. A suitable power source is required to produce an electric arc between 6000-120000°C which melts and vaporizes a metal rod in the region where arc is created. The vaporized metal is condensed and then dispersed by deionized water to produce nano-fluids. An advantage of one-step synthesis method is that nanoparticle agglomeration is minimized. But main problem is that only low vapor pressure fluids are compatible with such a process.

Two step method

Two-step preparation process is extensively used in the synthesis of nano-fluids by mixing base fluids with commercially available nano powders obtained from different mechanical, physical and chemical routes such as milling, grinding, and sol-gel and vapor phase methods. An ultrasonic vibrator or higher shear mixing device is generally used to stir nano powders with host fluids. The frequent use of ultra-sonication or stirring is required to reduce particle agglomeration. Two-step method can also be used for synthesis of carbon

nanotube based nano-fluids. Single-walled and multi-walled carbon nanotubes are first produced by pyrolysis method and then suspended in base fluids with or without the use of surfactants. Stability is a big issue inherently related to this operation as the powders easily aggregate due to strong van der Walls force among nanoparticles. In spite of such disadvantages this process is still popular as the most economic process for nano-fluids production.

1.5 Objective of the study

Objective of the study is to overcome the limitations of conventional engine coolant. Two commonly available nanoparticles (Al_2O_3 and TiO_2) were compared in terms of thermal performance and stability in the solution. In the present study conventional radiator is used with Al_2O_3 – Water based nano-fluid and following were the objectives of the study

- To develop a nano-fluid based engine coolant
- To conduct experiments on it using TiO_2-water and Al_2O_3–water nano-fluid and find appropriate nanomaterial for the purpose.
- To analyze the experimental data
- Determine various thermal performance parameters of radiator
    - Coolant heat rejection
    - Maximum temperature achieved
    - Comparison of thermal efficiency at different loads and different weight fraction of nanomaterial.
    - Heat balance of engine for the comparative study.

1.6 Organization of thesis

Chapter 1: Introduction

First chapter states the introduction of the automotive radiator and types of radiator systems used and advantages and limitations of liquid cooling. Objectives of the study are also included.

Chapter 2: Literature Review

In this chapter overview of the available literatures corresponding to the radiator (Theoretical and experimental study at the world and Indian level) has been discussed. Also the literatures on nano-fluid properties and preparation are also discussed. Observations are given for using this knowledge in the present study.

Chapter 3: Experimental Study

This chapter includes step by step installation of liquid cooling experimental setup and procedure for experimentation. The properties and preparation methods are also discussed in this chapter. The brief explanation of the instruments used is discussed.

Chapter 4: Data collection and Result Analysis

It includes the experimental plan and data tables for every concentration and corresponding performance curves. It also includes the comparative analysis of the performance at various loads and various weight fractions of nano-fluids.

Chapter 5: Conclusion

The conclusions are summarized in this chapter. Future developments are suggested and scope of future work is indicated.

Chapter 2 Literature review

A detailed literature is available on applications of nanofluids. But most of the studies are on standalone/isolated radiators, a few studies on direct engine application are available. A detailed review of different mathematical, experimental and theoretical studies is presented in this chapter.

2.1 Studies on nanofluids

Xuan et al. (2000) [1] suggested various methods of preparing different nanofluids with different base fluids. The most effective methods used for preparation of suspensions: (1) to change the pH value of suspensions; (2) to use surface activators and/or dispersants; (3) to use ultrasonic vibration were suggested in the paper. They suggested that The volume fraction, shape, dimensions and properties of the nanoparticles affect the thermal conductivity of nanofluids. Some correlations regarding Nusselt number has also been arrived at. The ratio of the thermal conductivity of the nanofluid to that of the base liquid varies from 1.24 to 1.78 if the volume fraction of the ultrafine particles increases from 2.5% to 7.5%.

Keblinski et al. (2002) [2] suggested various theories regarding increase in thermal conductivity with decreasing in particle size and increasing concentration. Four possible explanations were examined which are, Brownian motion, Molecular level layering, nature of heat transport and effects of nanoparticle clustering. Ballistic effects have been found more profound in enhancing the thermal conductivity rather than diffusive elements. The need of computer simulation has been discussed.

Mujumdar et al. (2006)[3] presented a review of heat transfer characteristics. The main focus is on the role of convective heat transfer in forced and free convection conditions. They prepared theoretical models for viscosity and thermal conductivity calculations. They further suggested that particle–liquid interaction and the movement between the particle and liquids play important roles in affecting the convective heat transfer performance of nanofluids.

Mintsa et al. (2007)[4] They presented the way of effective thermal conductivity measurements of alumina/water and copper oxide/water nanofluids. Effect of volume fraction, temperature and particle size was investigated. Readings were taken at ambient temperature as well as over a relatively large temperature range for various particle volume fractions up to 9%. Relative increase in thermal conductivity was found to be more at higher temperatures.

Duangthongsuk et al. (2009) [5] They investigated the thermal conductivity and viscosity of TiO_2 nanofluid with volume concentration ranging from 0.2 to 2 %. A transient hot-wire apparatus is used for measuring the thermal conductivity of nanofluids whereas the Bohlin rotational rheometer (Malvern Instrument) is used to measure the viscosity of nanofluids. The temperature range of the experiment was 15 to 35°C. The results show that the measured viscosity and thermal conductivity of nanofluids increased as the particle concentrations increased and are higher than the values of the base liquids. Thermal conductivity of nanofluids increased with increasing nanofluid temperatures and, conversely, the viscosity of nanofluids decreased with increasing temperature of nanofluids. The measured thermal conductivity and viscosity of nanofluids are different from the predicted values from the existing correlations and the data reported by other researchers. The new thermo physical correlations are proposed for predicting the thermal conductivity and viscosity of nanofluids.

Chen et al. (2009) [6] A methodology is proposed for predicting the effective thermal conductivity of dilute suspensions of nanoparticles (nanofluids) based on rheology. This methodology uses the rheological data to infer microstructures of nanoparticles quantitatively.

It was then incorporated into the Hamilton–Crosser equation to predict the effective thermal conductivity.

The methodology is validated experimentally by using four different type of nanofluids made of TiO_2 nanoparticles and titanate nanotubes dispersed in water and ethylene glycol. It is concluded that the modified Hamilton–Crosser equation successfully predicted the effective thermal conductivity of the nanofluids.

Wen et al. (2009) [7] This paper presents critical review of research on heat transfer applications of nanofluids with the aim of identifying the limiting factors so as to push forward their further development. They argued that most current research is still focused on thermal conductivity, neglecting the alteration of other properties by nanofluids especially viscosity and surface properties. Effect on boiling heat transfer has also been discussed. An in-depth understanding of the interactions between particles, stabilizers, the suspending liquid and the heating surface will be important for applications. Inter-disciplinary collaboration among nanomaterials, colloid science, physics and engineering researchers will be necessary to engineer suitable nanofluids and accelerate their applications.

Sundar et al. (2013) [8] Experimental investigations and theoretical determination of effective thermal conductivity and viscosity of magnetic Fe_3O_4-water nanofluid were reported in this paper. The nanofluid was prepared by synthesizing Fe_3O_4 nanoparticles using the chemical precipitation method, and then dispersed in distilled water using a sonicator. Both experiments were conducted in the volume concentration range 0.0% to 2.0% and the temperature range 20 °C to 60 °C. The thermal conductivity and viscosity of the nanofluid were increased with an increase in the particle volume concentration.Simple correlations were developed for the estimation of thermal conductivity and viscosity by considering particle volume concentration and temperature based on the experimental data.

Farooky et al. (2013) [9] Thermal conductivity of ethylene glycol and water mixture based Al_2O_3 and CuO nanofluids has been estimated experimentally at different volume concentrations and temperatures. The base fluid is a mixture of 50:50% (by weight) of ethylene glycol and water (EG/W). The particle concentration up to 0.8% and temperature range from 15°C–50°C were considered. Both the nanofluids are exhibiting higher thermal conductivity compared to base fluid. Under same volume concentration and temperature, CuO nanofluid thermal conductivity is more compared to Al_2O_3 nanofluid. A new correlation was developed based on the experimental data for the estimation of thermal conductivity of both the nanofluids. Since the nanofluids

exhibit enhanced thermal conductivity with an increase in temperature, it is concluded that their application in higher temperature environment will be more beneficial.

Khedkar et al. (2014) [10] Heat-transfer characteristics of TiO_2–water nanofluids as a coolant in concentric tube heat exchanger are presented in this paper. The heat exchanger is fabricated from copper concentric inner tube with length 1 m. The nanofluid is the mixture of water as base fluid and TiO_2 particles in nano size. The results obtained from the nanofluids cooling in concentric tube heat exchanger are compared with those from base fluids (water) as coolant. Effects of inlet flow rate of hot fluids, Reynold's number and composition of nanofluids on concentric tube heat exchanger are considered. It is observed that the average heat transfer rates for nanofluids as a cooling media are higher than those for the water which is also used as cooling media, and this increases with concentration of nanofluid composition. The results of this study have technological importance for the efficient design of concentric tube heat exchanger to enhance cooling performance at low heat flux cooling systems.

Maddah et al. (2014) [11] They studied fluid flow of the Al_2O_3 nanofluid for a range of Reynolds number (5000 to 21,000) with a range of solid volume fraction (0.2% to 0.9%).in a horizontal double pipe heat exchanger fitted with modified twisted tapes under turbulent flow conditions. The thermal performances of the heat exchanger with nanofluid and modified twisted tapes were evaluated for the assessment of overall improvement in thermal behaviour.

Generalized correlations were developed for the estimation of Nusselt number, friction factor and thermal performance factor under turbulent flow conditions. Satisfactory agreement between the present correlations and obtained experimental data validate the proposed correlations.

Zhang et al. (2014) [12] They investigated TiO_2–water nanofluid single-phase flow and heat transfer characteristics in a multiport minichannel flat tube with a 1.65 mm hydraulic diameter experimentally. TiO_2 nanoparticles with nominal diameters of 10, 30, and 50 nm were used at various volume concentrations ranging from 0.005% to 1% dispersed in water.

The friction factor and Nusselt number of the nanofluids were tested and compared with those of the base fluid, the Reynolds number of which varied from 100 to 6100. Results indicated that friction factor and Nusselt number of the nanofluids were higher than those of water. Both nanofluid density and particle migration significantly affected friction factor. Nanofluids at 0.01% concentration with diameter = 10 nm exhibited the best performance on the basis of the evaluation criterion, which considered heat transfer enhancement at the consequence of increased friction factor.

Sheikholeslami et al. (2015) [13] In this paper the problem of nanofluid hydrothermal behaviour in presence of variable magnetic field is investigated analytically using Differential Transformation Method. The fluid in the enclosure is water containing different types of nanoparticles: Al_2O_3 and CuO. The effective thermal conductivity and viscosity of nanofluid are calculated by KKL (Koo–Kleinstreuer–Li) correlation. The effect of Brownian motion on the effective thermal conductivity is considered. The effect of the squeeze number, nanofluid volume fraction, Hartmann number and heat source parameter on flow and heat transfer is investigated. The results show that skin friction coefficient increases with increase of the squeeze number and Hartmann number but it decreases with increase of nanofluid volume fraction.

Reddy et al. (2014) [14] Heat transfer coefficient and friction factor of TiO_2 nanofluid flowing in a double pipe heat exchanger with and without helical coil inserts are studied experimentally. The experiments are conducted in the range of Reynolds number from4000 to 15,000 and in the volume concentration range from 0.0004% to 0.02%. The base fluid is prepared by considering 40% of ethylene glycol and 60% of distilled water. The heat transfer coefficient and friction factor get enhanced by 10.73% and 8.73% for 0.02% volume concentration of nanofluid when compared to base fluid flowing in a tube. Heat transfer coefficient and friction factor further get enhanced by 13.85% and 10.69% respectively for 0.02% nanofluid when compared to base fluid flowing in a tube with helical coil inserts. Based on the experimental data, generalized correlations are proposed for Nusselt number and friction factor. The results are presented in graphical and tabular form. Uncertainty analysis is also carried out and the experimental error is in the range of ±10%.

Sonawane et al (2014) [15] This paper presents experimental and theoretical determination of the effective thermal conductivity of various base fluids and nano TiO_2 composition.TiO_2 nanoparticles having an average diameter of 5 nm with variation in volume concentrations from 1% to 6% nanofluids were prepared using a two-step method under sonication and without any surfactant addition.

Water-based nanofluids provide the highest thermal conductivity enhancement of 22% as compared to other base fluids. The thermal conductivity data were generated by using a model for comparison with experimental data, which show that ethylene glycol and paraffin oil nanofluids thermal conductivity were in good agreement with those of the Bruggeman model.

2.2 Experimental works on Radiators with Nanofluids

Kulkarni et al. (2007) [16] This paper presents a study on nanofluids applications, such as a coolant in a diesel electric generator (DEG). Specific heat measurements of aluminium oxide nanofluid with various particle concentrations have been presented demonstrating a reduction in their values with an increase in the particle concentration and an increase with temperature. Experiments were performed on the DEG to assess the effect of nanofluids on cogeneration efficiency. The investigation showed that applying nanofluids resulted in a reduction of cogeneration efficiency. This is due to the decrease in specific heat, which influences the waste heat recovery from the engine. However, it was found that the efficiency of waste heat recovery heat exchanger increased for nanofluid, due to its superior convective heat transfer coefficient.

Saidur et al. (2010) [17] This study focused on the application of ethylene glycol based copper nanofluids in an automotive cooling system. Relevant input data, nanofluid properties and empirical correlations were obtained from literatures to investigate the heat transfer enhancement of an automotive car radiator operated with nanofluid-based coolants. It was observed that, overall heat transfer coefficient and heat transfer rate in engine cooling system increased with the usage of nanofluids (with ethylene glycol the base fluid) compared to ethylene glycol (i.e. base fluid) alone. It is observed that, about 3.8% of heat

transfer enhancement could be achieved with the addition of 2% copper particles in a base fluid at the Reynolds number of 6000 and 5000 for air and coolant respectively. In addition, the reduction of air frontal area was estimated to be 18.7%.

Hashemabadi et al. (2011) [18] In this paper, the heat transfer performance of pure water and pure EG has been compared with their binary mixtures. Furthermore, different amounts of Al_2O_3 nanoparticle have been added into these base fluids and its effects on the heat transfer performance of the car radiator have been determined experimentally. Liquid flow rate has been changed in the range of 2–6 l per minute and the fluid inlet temperature has been changed for all the experiments. The results demonstrate that nanofluids clearly enhance heat transfer compared to their own base fluid. In the best conditions, the heat transfer enhancement of about 40% compared to the base fluids has been recorded. Reduced radiator sizing has also been discussed.

Hussein et al. (2014) [19] In this paper, heat transfer enhancement using TiO_2 and SiO_2 Nano powders suspended in pure water is presented. The test setup includes a car radiator, and the effects on heat transfer enhancement under the operating conditions are analyzed under laminar flow conditions. The volume flow rate, inlet temperature and nanofluid volume concentration are in the range of 2–8 lpm, 60–80 °C and 1–2% respectively. The results showed that the Nusselt number increased with volume flow rate and slightly increased with inlet temperature and nanofluid volume concentration. The regression equation for input (volume flow rate, inlet temperature and nanofluid volume concentration) and response (Nusselt number) was found. The results of the analysis indicated that significant input parameters to enhance heat transfer.

Theoretical works nanofluids

Mahian et al. (2013) [20] presented their review on the application of nanofluids in solar energy. Therefore, a major part of this review paper allocated to the effects of nanofluids on the performance of solar collectors and solar water heaters from the efficiency, economic and environmental considerations viewpoints. In addition, some reported works on the applications of nanofluids in thermal energy storage, solar cells, and solar stills are reviewed. Subsequently, some suggestions are made to use the nanofluids in different solar thermal

systems such as photovoltaic/thermal systems, solar ponds, solar thermoelectric cells, and so on. Finally, the challenges of using nanofluids in solar energy devices are discussed.

Ghadimi et al. (2013) [21] investigated the stability of titania nano-suspensions by comparing the effect of surfactant addition and ultrasonic processing. In this study, six different nanofluids with 0.1 wt.% loading of TiO_2 nanoparticles (25 nm diameter) were prepared using a two-step method. Ultrasonic processing (i.e. bath and horn) were applied to help the homogeneity and Sodium Dodecyl Sulfate (SDS) as anionic surfactant was added to monitor the stability of the samples. Transmission Electron Microscopy (TEM) and sedimentation photo capturing were applied to visualize the stability and sedimentation rate of the prepared nanofluids. In addition, thermal conductivity and viscosity of these six samples were measured. The results revealed that 3-h ultrasonic bath process with the addition of 0.1 wt.% of surfactant can be the most stable suspension with the highest thermal conductivity for further applications within 1 month.

Ghanbarpour et al. (2014) [22] performed experimental and theoretical study of thermal conductivity and viscosity of Al_2O_3/water nanofluids. Various suspensions containing Al_2O_3 nanoparticles were tested in concentration ranging from 3% to 50% in mass and temperature ranging from 293 K to 323 K. The results reveal that both the thermal conductivity and viscosity of nanofluids increase with temperature and particle concentration accordingly while the increase in viscosity is much higher than the increase in thermal conductivity. The thermal conductivity and viscosity enhancement are in the range of 1.1–87% and 18.1–300%, respectively. Moreover, the results indicate that the thermal conductivity increases nonlinearly with concentration, but, linearly with the increase in temperature. In addition, the experimental results are compared with some existing correlations from literature and some modifications are suggested.

Yoo et al. (2007) [23] studied the thermal conductivity of Al_2O_3 nanofluids and compared with that of Fe nanofluids. Al_2O_3 nanofluids show thermal conductivity close to the value predicted by the H-C model, while the thermal conductivity of Fe nanofluids is improved more than as predicted by the H-C model. pH effect on thermal conductivity is also done in this study. It is observed that thermal conductivity increase with changes in pH.

Sidik et al. (2014) [24] discussed nanofluid preparation methods based on available literature. To prepare nanofluids, three methods have been used: 1) Sonication: it was shown that sonication time has an effect on the zeta potential and nanoparticle sizes. Some nanofluids were sonicated just to be kept stable for the duration of the experiment, which limits the commercialization of nanofluids. 2) pH control: the value of zeta potential is generally obtained by adjusting the pH value according to just one small volume fraction value even though the particle volume fraction affects the zeta potential, i.e., pH value.

3) Surfactants: a critical micelle concentration should be respected to avoid the speedy sedimentation of nanoparticles. They found that an optimum amount of surfactant and pH value can be found to keep the physical properties constant.

Xia et al. (2014)[25] showed effect of two kinds of surfactants d sodium dodecyl sulphate (SDS) and polyvinylpyrrolidone (PVP) d on the stability and thermal conductivity of Al2O3/de-ionized water nanofluids are analyzed respectively. Results show that surfactant plays an important role in dispersing the nanoparticles into the base fluid and improving the stability of Al2O3/de-ionized water nanofluids. Non-ionic surfactant PVP shows better positive effects than anionic surfactant SDS on the dispersion and stability of the nanofluids. The highest thermal conductivity occurred at an optimal concentration ratio of surfactant mass fraction and particle volume fraction, where the ratio is partly associated with the particle size and decreases with the increase of particle volume fraction.

Li et al. (2008)[26] showed that the thermal conductivity enhancements of Cu-H_2O nanofluids are highly dependent on the weight fraction of nanoparticle, pH values and SDBS surfactant concentration of nano-suspensions. The Cu-H_2O nanofluids with an ounce of Cu have noticeably higher thermal conductivity than the base fluid without nanoparticles, For Cu nanoparticles at a weight fraction of 0.001 (0.1 wt.%), thermal conductivity was enhanced by up to 10.7%, with an optimal pH value and SDBS concentration for the highest thermal conductivity. Therefore, the combined treatment with both the pH and chemical surfactant is recommended to improve the thermal conductivity for practical applications of nanofluid.

2.3 Observations and Recommendations based on Literature Review

Following are the observations on the basis of literature study

- The performance of radiator collector is improved by 15-20% with the use of nanofluid as compared to base fluid.
- Thermal conductivity of nanofluid depends on various factors like volume fraction, nanoparticle size, morphology, additives, pH, temperature, nature of base fluid, nanoparticle material etc.
- The main problems associated with the nanofluid are agglomeration and stability.
- Only few experimental studies are available on radiator with nanofluid and the most of them are with standalone radiator type.
- The stability analysis has only visual basis, no quantitative studies has been carried out.

Following recommendations can be made on the basis of literature study

- To find out the actual performance of engine cooling system it is required to develop a complete experimental setup and measure the performance at different engine load and concentration of nanoparticles.
- Quantitative basis of stability is needed to be prepared to get actual trend of nanofluid stability.

Chapter 3 Experimental study

The basic principle of engine radiator is that working fluid flowing through the coolant jacket directly absorbs excess heat and heats up. The cooling fluid is then circulated through radiator tubes and exchange heat with the fins attached. These fins throw that heat to the ambient air. Development of experimental setup includes the procurement and installation followed by the experimental analysis in ambient conditions.

3.1 Setup Preparation and Installation

The setup consists of water cooled engine, coupling with pulley, radiator, hoses, water pump, radiator stand, fan, fan-belt etc. Installation of water cooling circuit has various steps that involve various components. The detailed photographic view of each component has been shown below.

3.1.1 Changing the coupling

The earlier cooling system used was “pass through” in which a large water reservoir was being used for cooling. The coupling between engine and alternator needed to be replaced in order to accommodate the provision for fan belt. One can easily see the added crank pulley which will drive the fan belt.

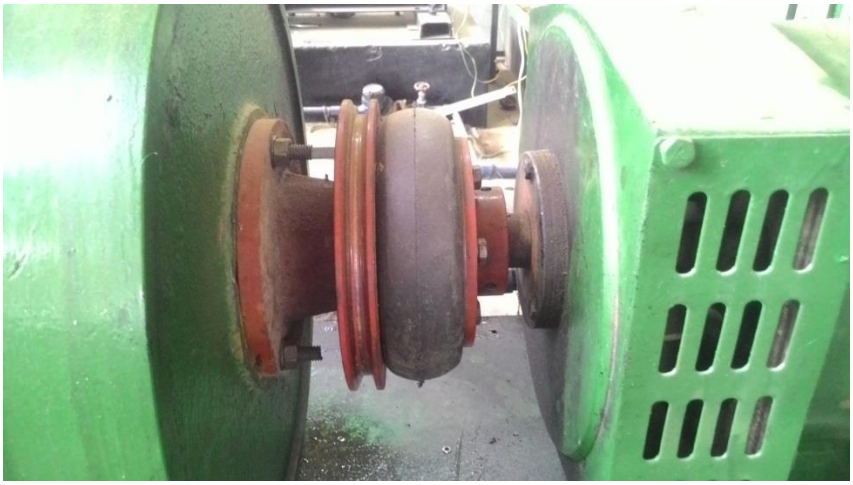

Figure 7: The new coupling

3.1.2 Installation of radiator stand

Radiator stand was prepared by joining several L sections together to provide adequate support to radiator. The figure below shows the lower part of the stand.

Figure 8: Radiator stand

The stand was fixed to the base by drilling holes in the base sheet and two sections were bolted to the base plate. One of them is shown in figure below.

Figure 9: Attachment to base plate

3.1.3 Radiator installation

Figure 10: Radiator installation

Radiator was installed on lower support columns to fix the location of upper support columns. Initially it was installed on temporary arrangement but as more support columns were in place, the radiator was fixed firmly on the base foundation.

The location of columns was so decided that radiator undergoes small amplitude harmonic vibrations which will prevent the nano-particles from coagulating and settling down to the base of radiator.

3.1.4 Upper support sections

The upper support sections were installed after the radiator was fixed to the lower support bars. The upper sections were installed to check the lateral swing of the radiator.

Figure 11: Upper support arms

Thermocouples were installed at exhaust manifold, water jacket inlet and outlet, inlet manifold and on engine body to monitor the engine temperature during the experiment. K-Type thermocouples were used at all thermocouple locations.

3.1.5 Water body and pump installation

Pump and water body assembly was installed on the engine on two of the main studs as shown in the figure. The hoses were connected at appropriate locations and fan-belt was fitted on the pump pulley. Radiator fan was installed in pump pulley with the help of four bolts.

Figure 12: water body with pump

3.1.6 Fan and fan belt

The fan belt is connected between crank pulley and pump pulley as shown in figure 13. The pump pulley is driven by crank pulley. The radiator fan is also attached to pump assembly and rotates with it in front of radiator. As the engine is constant speed type, therefore the fan always rotates at constant speed for all load conditions.

Figure 13: Fan belt installation

3.1.7 Water manifold (inlet and outlet) and hoses

Water manifolds were attached to the cylinder block. It is used to connect inlet and outlet hoses to and from the engine. The hoses were connected as shown and they are held with the help of hose clips. This prevented the leakage of coolant from the components. The hoses are made of rubber based material to ensure flexibility in operation. The hoses are able to bear the temperature in excess of 150°C which is perfect for the engine operation.

Figure 14: water manifolds and hoses

Complete experimental setup

Figure 15: Complete experimental setup

3.2 Specification of experimental setup

The setup consists of water cooled diesel engine, electric dynamometer radiator, hose pipe, water pump, hose clips, water bodies, radiator stand, fan-belt, fan etc. the specification of experimental setup are as follows:

3.2.1 Engine Specifications

Table 1 Engine Specifications

PARAMETER	UNIT/TYPE	SPECIFICATION
Rated output	kW (hp)	3.7 (5)
No of cylinders		1
Bore x stroke	mm	80 x 110
Compression ratio		22
Aspiration		Natural
Type		C.I
Fuel		High speed diesel
Injection type		Direct injection
Speed	constant speed	1500 rpm
Governor	Mechanical	Class B-1
Lubrication	Wet sump	SAE 30/SAE 40
SFC	gms/hp-hr	252
Cooling	Water cooling	Radiator cooled

3.2.2 Alternator Specifications

Table 2 Alternator specifications

PARAMETER	UNIT/TYPE	SPECIFICATION
TYPE		Slip ring type
No of poles		4
Speed	RPM	1500
Max output	kVA	5
Frequency	Hz	50 ± 5

Insulation class	H	180 °C
Phase		single
Power factor (P.F)		1
Efficiency	%	79 @ full load

3.2.3 Cooling apparatus specifications

Table 3 Cooling apparatus specifications

PARAMETER	UNIT/TYPE	SPECIFICATION
Model	TV-1/AV-1	Kirloskar
No of tubes		104
Pass		Vertical
Frontal area		30cm x 30 cm
Hose pipes	standard	
Pump assembly	standard	
Fan and fan belt	standard	

3.3 Procedure of experiment

The experiment was divided into two phases:

1) Determination of stability and selection of suitable nano-fluid among aluminum oxide and titanium dioxide.
2) Engine experimentation with nano-fluid selected from above experiment.

The first phase has following procedure:

1. Preparation of nano-fluid in required concentration.
2. Ultrasonic vibration for sonication time duration.
3. Storage in undisturbed container after sonication.
4. Maintain constant temperature conditions.
5. Measurement of thermal conductivity and visual inspection at regular interval.
6. Record thermal conductivity of undisturbed nano-fluid.
7. Plot the records in a graph.

The Second phase has following procedure:

1. Start the engine and let it idle for 15 minutes to ensure temperature stability.
2. Take relevant readings of all temperatures, coolant, fuel and air flow rates.
3. Increase the load in gradual steps, let it run till temperatures stabilizes.
4. Repeat above two steps for all loads.
5. Run the engine at idle for 10 minutes to cool down, then shut down the engine.
6. Repeat above procedure for different concentrations.
7. Draw heat balance for all concentrations.
8. Compare the results and find favorable case.

3.4 Nano-fluid preparation and its properties

Nano-fluid is a fluid containing nanometer sized particles with at least one of their dimensions smaller than 100 nm, called nanoparticles. These particles are dispersed in a base fluid like water, ethylene glycol and/or oil. The nanoparticles used in nano-fluids are made of metals, oxides, carbides, or carbon nanotubes. Nano-fluid are two phase system with one solid phase (nanoparticles) another liquid phase (base fluid). Nano-fluids have been found to enhanced thermo-physical properties such as thermal conductivity, thermal diffusivity, viscosity and convective heat transfer coefficients compared to those of base fluids.

Nano-fluids have novel properties that make them potentially useful in many applications in heat transfer, including microelectronics, fuel cells, solar water heating, cooling of transformer oil, pharmaceutical processes, and hybrid powered engines, engine cooling/vehicle thermal management, domestic refrigerator, improving heat transfer efficiency of chillers, heat exchanger, nuclear reactor coolant, in grinding, machining, in space technology, defense and ships, and in boiler flue gas temperature reduction.

3.5 Properties of Nano-fluid

The models used for calculating the properties of nano-fluids [23] are as follows:

1. Density

The density of nano-fluid is based on the physical principle of the mixture rule. As such it can be represented as:

$$\rho_{eff} = \left(\frac{m}{V}\right)_{eff} = \frac{m_f + m_p}{V_f + V_p} = \frac{\rho_f V_f + \rho_p V_p}{V_f + V_p} = (1 - \emptyset_p)\rho_f + \emptyset_p \rho_p \text{.....(3.1)}$$

Where,
ρ_{eff}= effective density of nano-fluid
ρ_f = density of fluid
ρ_p = density of particle
m_f = mass of fluid
m_p = mass of particle
V_f = volume of fluid
V_p = volume of particle
Φ_p= volume fraction of particle

2. Heat capacity

The specific heat of nano-fluid can be determined by assuming thermal equilibrium between the nanoparticles and the base fluid and given as follows:

$$C_{eff} = \frac{\{(1-\emptyset_p)\rho_f c_f + \emptyset_p \rho_p c_p\}}{\rho_{eff}} \text{.....(3.2)}$$

Where,
C_{eff}= heat capacity of nanofluid
C_f = heat capacity of fluid
C_p = heat capacity of particle

3. Thermal expansion coefficient

Thermal expansion coefficient of nano-fluids can be estimated utilizing the volume fraction of the nanoparticles on the weight basis as follows:

$$\beta_{eff} = (1 - \emptyset_p)\beta_f + \emptyset_p \beta_p \text{.....(3.3)}$$

Where,
β_{eff} = thermal expansion coefficient of nano-fluid
β_f = thermal expansion coefficient of fluid

β_p = thermal expansion coefficient of nanoparticle

4. Thermal conductivity

Thermal conductivity of nano-fluid is given by the following formula:

$$k_{eff} = k_f + \left[\frac{3\emptyset_p(k_p - k_f)}{k_p + 2k_f - \emptyset_p(k_p - k_f)}\right] \quad \text{.....(3.4)}$$

Where,
k_{eff} = thermal conductivity of nanofluid
k_f = thermal conductivity of fluid
k_p =thermal conductivity of nanoparticle

5. Effective viscosity

Effective viscosity of nano-fluid is given by following relation:

$$\mu_{eff} = (1 + 5.45\emptyset_p + 108.2\emptyset_p^2)\mu_f \quad \text{.....(3.5)}$$

Where,
μ_{eff} = viscosity of nanofluid
μ_f = viscosity of fluid

6. Volume fraction

Volume fraction of nano-fluid is given as

$$\emptyset_p = \frac{m_p}{(V_f + V_p)\rho_p} \times 100 \quad \text{.....(3.6)}$$

3.6 Material Properties

Table 4 Properties of various nanoparticles

Class of Nanomaterial	Nanomaterial	Thermal conductivity (W/m-K)	Density (kg/m^3)	Specific heat (kJ/kg-K)
Metallic	Silver	429	10490	0.23
	Copper	401	8940	0.39
	Gold	316	19312	0.13
	Aluminum	237	2712	0.91
	Zinc	116	7135	0.39
	Titanium	21.9	4500	0.54
Non metallic	Alumina (Al_2O_3)	40	3950	0.765
	CuO	20	6500	0.535
	ZnO	21	5610	0.635
	Titania (TiO_2)	8.4	4250	0.692

Table 5 Properties of base fluids

S. No.	Base fluid	Thermal conductivity (W/m-K)	Density (Kg/m^3)	Specific heat (kJ/kgK)
1	Water	0.609	1000	4.178
2	Ethylene glycol	0.258	1097	2.36
4	Acetone	0.18	784.6	2.15

Table 6 Properties of TiO_2-Water nano-fluid at different volume fractions

Nanoparticle	Volume fraction of NP (%)	Effective density of nanofluid (kg/m^3)	Heat capacity (kJ/kg-K)	Thermal conductivity (W/m-K)
TiO_2	0.0	1000.00	4.178	0.609
	0.2	1001.532	4.171174	0.610146
	0.4	1003.068	4.164348	0.611296
	0.6	1004.609	4.157522	0.612451
	0.8	1006.155	4.150696	0.61361
	1.0	1007.706	4.14387	0.614773

Table 7 Properties of Al_2O_3 –Water-Nanofluid at different volume fractions

Nanoparticle	Weight fraction of NP (%)	Effective density of nanofluid (kg/m^3)	Heat capacity (kJ/kg-K)	Thermal conductivity (W/m-K)
Al_2O_3	0.0	1000.00	4.178	0.609
	0.2	1001.515	4.171087	0.610473
	0.4	1003.035	4.164174	0.611952
	0.6	1004.559	4.157261	0.613437
	0.8	1006.087	4.150349	0.614928
	1.0	1007.621	4.143437	0.616425

Variation of properties of nanofluid with change in volume concentration of nanoparticles is given in table 6 and 7 for TiO_2 and Al_2O_3 nanoparticles respectively. It is clear from tables with increase in volume concentration of nanoparticles in the fluid density and thermal conductivity increases but heat capacity of the fluid is decreases.

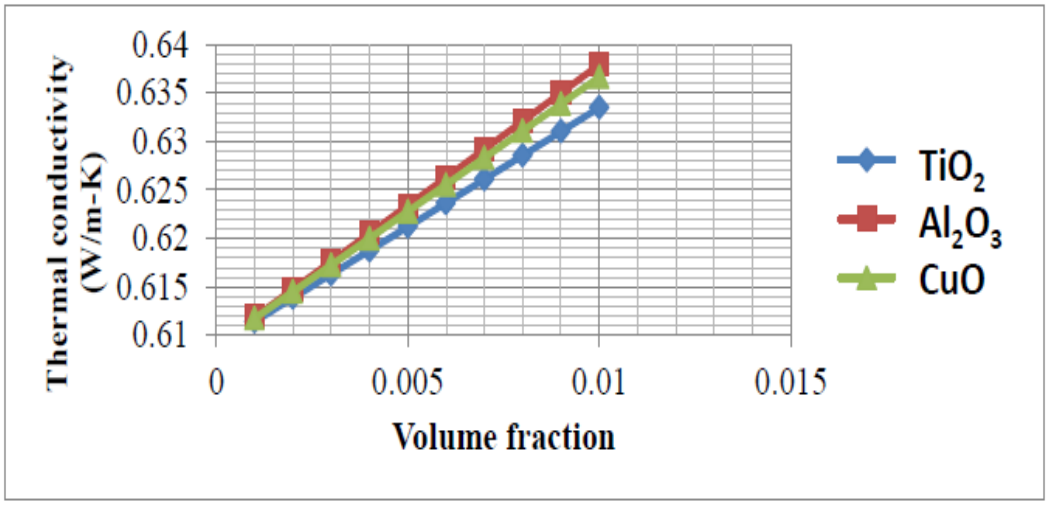

Figure 16 Variation of thermal conductivity with volume fractions

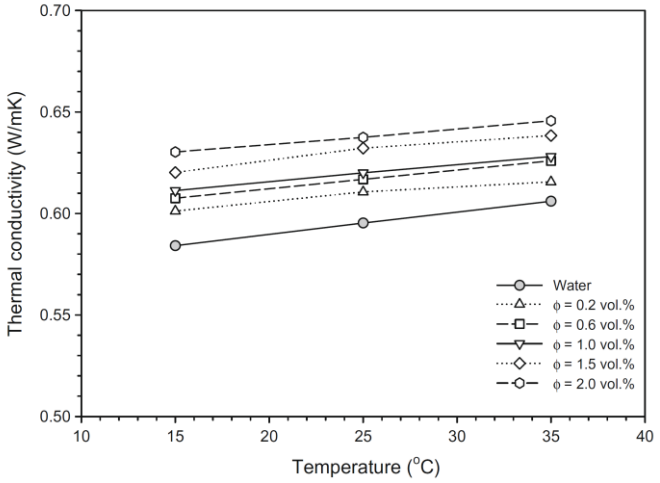

Figure 17 Effect of temperature and volume fraction on thermal conductivity of TiO_2-Water nanofluid [21]

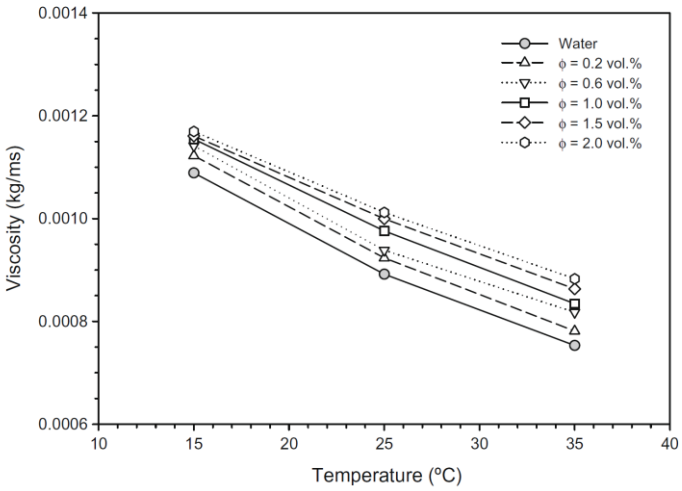

Figure 18 Effect of temperature and volume fraction on viscosity of TiO_2-Water nanofluid [21]

The effect of temperature and volume fraction of nanoparticle on thermal conductivity and viscosity for TiO_2-water nano-fluid are shown in figure 17 and 18 respectively. It is clear from figures that the thermal conductivity of nano-fluid increases with increase in temperature and volume fraction but viscosity of nano-fluid decreases with increase in temperature and decrease in volume fraction. The variation is almost linear in both the cases.

3.7 Preparation of nano-fluid

Preparation of nano-fluids is an important step. In general, it consists of two methods [22]:

I. Two step method
II. One step method

3.7.1 Two step method

Two-step method is the most widely used method for preparing nanofluids. Nanoparticles, nano-fibers, nanotubes or other nano-materials used in this method are first produced as dry powders by chemical or physical methods. Then the nano sized powder will be dispersed into a fluid in the second processing step. For second step there are various methods used as follows:

- Intensive magnetic force agitation
- Ultrasonic agitation
- High shear mixing
- Homogenizing
- Ball milling

Two step method is the most economical method to produce nanofluids because nano powder synthesis techniques have already been scaled up to industrial production. Due to the difficulty in preparing stable nano-fluids by two step method, several advanced techniques are developed to produce nanofluids.

3.7.2 One step method

The one-step process consists of simultaneously making and dispersing the particles in the fluid. In this method the processes of drying, storage, transportation, and dispersion of nanoparticles are avoided, so the agglomeration of nanoparticles is minimized and the stability of fluids is increased. The one step process prepares uniformly dispersed nanoparticles and the particles can be stably suspended in the base fluid.

One-step physical method cannot synthesize nanofluids in large scale and the cost is also high, so the one-step chemical method is developing rapidly.

We utilized the two step method for nanofluid preparation due to its availability at the laboratory.

3.7.3 Mass of nanoparticles required

For preparation of nano-fluid mass of nanoparticle required depends upon the weight fraction of nanoparticle in nano-fluid. Mass of nanoparticle is calculated as

Mass of nanoparticle = volume of nanofluid x density of nanoparticle x volume fraction

For 5 liters of TiO_2-Water nano-fluid, mass of nanoparticles (TiO_2) required for different weight fractions are given in table 8

Table 8 Mass of TiO_2 required for various weight fractions for 5 litre nanofluid

Nanoparticle	Weight Fraction (%)	Mass of Nanoparticle (gm)
TiO_2	0.0	0
	0.2	10.01532
	0.4	20.06136
	0.6	30.13828
	0.8	40.24621
	1.0	50.3853

Similar calculations were done for Aluminum oxide nanoparticles and following table represents the quantity.

Table 9 Mass of Al_2O_3 required for various weight fractions for 5 litre nanofluid

Nanoparticle	Weight Fraction (%)	Mass of Nanoparticle (gm)
Al_2O_3	0.0	0
	0.2	10.01489
	0.4	20.05966
	0.6	30.13445

	0.8	40.23937
	1.0	50.37458

In the present study TiO_2 and Al_2O_3 nanoparticles and distilled water as a base fluid are used one at a time. The nano-fluid was prepared using two step method. The nanoparticles were suspended using Ultrasonic agitation. To prepare nano-fluid the nanoparticles were mixed with distilled water and subjected to ultrasonic vibration (600 W and 20 kHz) for 3-5 hours [24]. Mass of nanoparticles required for nano-fluid preparation of five different weight concentrations 0.1%, 0.2%, 0.4%, 0.6%, 0.8% and 1.0% are given in table 8 and 9.

From the literature review it is clear that the thermal conductivity increases with increase in volume/weight fraction of nanoparticles, but the problem of stability and agglomeration occurs.

In present study we used TiO_2 and Al_2O_3 nanoparticles of average size 30 nm. An ultrasonic vibrating machine of 600W and 20 kHz was used. The capacity of ultrasonic cleaner was 45 liters. But in our case we prepared only 5 liters nano-fluid as per the requirement of experimentation and capacity of radiator. The photographic view of ultrasonic cleaner is shown in figure 19.

Figure 19 Ultrasonic cleaner with 45 litre capacity

3.8 Stability Analysis of nano-fluid

The major problem associated with nano-fluid is its stability. There are various methods for nano-fluid preparation as mentioned earlier but still it is a challenge to prepare a nano-fluid

homogeneous and long term stable with negligible agglomeration, and without affecting the thermo-physical properties.

The stability analysis part of experimentation was divided into two parts namely determination of sonication time and stability measurement. The sonication time was determined by the following procedure:

1) Required quantity of nanoparticles was mixed with distilled water.
2) The mixture was agitated in ultrasonic vibrator (sonicator).
3) Small quantity of nano-fluid (100 ml) was drawn out at regular intervals.
4) The drawn out mixture was allowed to attain room temperature.
5) Thermal conductivity was measured with the help of KD2 pro instrument.
6) Steps 3, 4, 5 were repeated every 20 minutes in case of TiO_2.
7) Same experiment was repeated for Al_2O_3 with readings every 30 minutes.
8) Different concentrations were tested this way and results were recorded.

The ultrasonic vibrator was run continuously during the experiment. The thermal conductivity of the nano-fluid keeps on increasing with time as more particles becomes colloidal in nature. A time came when thermal conductivity no longer increased and became maximum.. After this point thermal conductivity started decreasing. The point of maximum thermal conductivity is called sonication time of particular nanofluid. It is different for different nanofluids.

As experiment was carried out for 5 to 6 hours in a day, so the nanoparticles remain suspended in the base fluid for at least 10-12 hours after experiment. The particle settlement was observed the next day in the test container. Although it is clear that thermal property have deteriorated but there is no quantitative basis for how much the thermal properties have decreased per unit time.

The stability analysis methodology provided by literature review was visual inspection at each concentration at regular intervals. The method chosen for this experiment is quantitative one. Instead of visual inspection, thermal conductivity of undisturbed sample of nanofluid was measured at regular intervals starting from just after sonication time was over.

This method provided a quantity based results for variation of thermal conductivity with time if nanofluid was kept undisturbed for certain duration. These readings are also taken with the help of KD2 pro instrument. The most important parameter to be controlled was temperature of the nanofluid. As thermal conductivity is very sensitive to temperature, for direct comparison it is very important to keep temperature variation in check.

Both the above mentioned experiments were done with above mentioned nanoparticles. The nanoparticles with superior properties, especially stability was be chosen for further experimentation on the engine radiator.

3.9 Engine operation and flow rate control

The fluid flow rate is very important parameter, as the performance of radiator depends on flow of fluid. In the present study the flow rate was constant due to constant engine speed and flow rate was measured using the pitot tube method. In this method a L shaped glass tube is installed on the outer part of the uppermost hose linked from the water jacket of the engine and the radiator. The fluid rises in the tube and gives direct measure of kinetic head from which velocity is determined and hence the mass flow rate

3.10 Calculations

The heat balance of engine best describes the capacity of the radiator to transfer thermal energy from the engine. Efficiency of radiator can vary depending on the coolant temperature, and ambient temperature. Heat balance is calculated from the following equation.

Heat input to engine = (Brake output + Exhaust heat loss + Coolant heat loss + Body heat loss + other losses)

Heat input to engine: It is the heat content provided by the fuel to the engine. Mathematically it is equal to the mass flow rate of fuel multiplied by calorific value of fuel (diesel in this case).

$$H = \dot{m}f * CV$$

Brake Output: It is measured with the help of a dynamometer. There are various types of engine dynamometers to measure the engine output. The discussion about dynamometers is beyond this topic. An electrical dynamometer was used in our experimentation, coupled to the engine.

The output of engine is measured by calculated the power output of the given alternator electric dynamometer). The alternator is loaded with the help of electric bulbs and energy output is measured by the help of voltmeters and ammeters.

$$BP = V * I * \frac{pf}{\eta}$$

Where V= voltage , I= current, p.f= power factor, η= alternator efficiency

Exhaust heat loss: It refers to the heat carried away in the hot exhaust gases leaving through exhaust port. The exhaust gas has a temperature range of 150°C to 500°C. The high temperature exhaust gases leaving unused represents the heat loss.

The rate of exhaust heat loss is given by-

$$He = \dot{m} * Cp * \Delta T$$

Where, m= gas mass flow rate (air + fuel)

Cp= specific heat of air (at constant pressure)

ΔT= temperature difference of exhaust gas and ambient air.

Coolant heat loss: It is the portion of heat carried away form the engine in the form of heated coolant. The metallurgic constraints limit the maximum operating temperature of the engine. The coolant temperature lies in the range of 55°C to 75°C in case of single cylinder engines of 5 hp capacity.

It is given by-

$$Hc = m\dot{c} * Cpc * \Delta T$$

Where- m_c- mass flow rate of coolant

Cpc – specific heat of coolant

ΔT= temperature difference between radiator inlet and outlet temperature

Body heat loss: When the engine is operational the metallic components gets heated. The heated body loses heat through convection and negligible amount through radiation.

Body loss is given by-

$$Hb = h * A * \Delta T$$

Where- h- convective heat transfer coefficient

A- surface area of the engine

ΔT= temperature difference between engine body and ambient temperature

The value of "h" can be found from following empirical relation.

$$h = 10.45 - v + 10\, v^{\frac{1}{2}}$$

v – air velocity (m/s)

Frontal area reduction

$$Hc = U * A * \Delta T$$

$$Hc \propto A$$

$$\frac{Hc1}{Hc2} = \frac{A1}{A2}$$

Where Hc= coolant heat loss

A= radiator frontal area

Hc_1, Hc_2, A_2 are known, A_1 can be calculated.

3.11 Instrumentation

To find out the thermal performance of nano-fluid for cooling system some instruments are required to measure and record the experimental readings like temperature, solar intensity, wind velocity etc. the following instruments were used to measure and record these parameters.

- KD2 pro
- Thermocouples
- Anemometer
- Tachometer (non-contact)
- Pitot tube
- U-tube manometer with air box
- Fuel burette

3.11.1 KD2 pro

The KD2 Pro is a handheld device used to measure thermal properties. The KD-2 Pro package consists of a handheld controller and one sensor kit. The single needle sensors measure thermal conductivity and resistivity; while the dual-needle sensor measures thermal conductivity, resistivity, volumetric specific heat capacity and diffusivity. Due to availability of only single needle sensor we had only measured thermal conductivity and temperature, all other parameters were calculated by empirical relations.

Figure 20 KD-2 pro for thermal conductivity measurement

3.11.2 Thermocouples

The working principle of thermocouple is based on Peltier effect which states that when two dissimilar metals are joined together to form two junctions, and different temperature are produced on these junction then emf is generated within the circuit. The total emf generated the circuit depends on the metals used within the circuit as well as the temperature of the two junctions. The total emf or the current flowing through the circuit can be measured easily by the suitable device. Now, the temperature of the reference junctions is already known, while the temperature of measuring junction is unknown. The output obtained from the thermocouple circuit is calibrated directly against the unknown temperature. Thus the voltage or current output obtained from thermocouple circuit gives the value of unknown temperature directly.

There are various types of thermocouples are available in market like J, K, T, E, R, S, B etc. In the present study K (chromel-constantan) type thermocouples were used for water inlet, water outlet, exhaust gas and ambient temperature measurement. The temperature range and sensitivity K type thermocouples are -270 to 1370℃, 40 μV/℃.

Figure 21 K and J type thermocouples

3.11.3 Anemometer

An anemometer or wind meter is a device used for measuring wind speed, and is a common weather station instrument. The term is derived from the Greek word anemos, meaning wind, and is used to describe any air speed measurement instrument used in meteorology or aerodynamics. For the experiment purpose it was used to measure wind velocity across the radiator fins and engine block.

3.11.4 Tachometer (non-contact)

A tachometer (revolution-counter, tach, rev-counter, RPM gauge) is an instrument measuring the rotation speed of a shaft or disk, as in a motor or other machine. The device usually displays the revolutions per minute (RPM) on a calibrated analogue dial, but digital displays are increasingly common. The non-contact type digital tachometer was used in our experiment.

3.11.5 U-tube manometer with air box

This arrangement was used to measure the air velocity through an orifice of known area. The height difference between two tubes gives the velocity and when it is multiplied by area of orifice, it gives the volumetric flow rate or discharge. Discharge multiplied by density of air gives mass flow rate of air.

3.11.6 Burette

It is long cylindrical tube with markers on the side (in ml). When fuel contained in the tube is made to flow to the engine we can measure the time for say 20ml fuel consumption. Dividing volume consumed by time gives fuel consumption in ml/sec.

Chapter 4 Data Collection and Result Analysis

Data were collected for radiator cooling system under various testing conditions i.e. at different engine loads and different weight fraction of nanoparticles in nano-fluid.

The data for following parameters was collected:

- Thermal conductivity
- Sonication time
- Inlet temperature of fluid (T_i)
- Outlet temperature of fluid (T_o)
- Engine body temperature at three different points (T_1, T_2 and T_3)
- Exhaust gas temperature (T_{eg})
- Ambient temperature (T^a)
- Air, Fuel and Coolant flow rate (m_a, m_f and m_c)

4.1 Experimental Plan

First Phase: Experimental study with TiO_2-water and Al_2O_3- water nanofluid at ambient temperature.

TiO_2-Water nanofluid

Day 1: TiO_2-water nanofluid (0.002 volume %)

Day 2: TiO_2-water nanofluid (0.004 volume %)

Al_2O_3- Water nanofluid

Day 1: Al_2O_3- water nanofluid (0.002 volume %)

Day 2: Al_2O_3- water nanofluid (0.004 volume %)

Second Phase: Experimental study with water cooled engine at constant flow rate at all loads

Day 1: Ethylene Glycol- water

Day 2: Al_2O_3- coolant nanofluid (0.1% weight fraction)

Day 3: Al_2O_3- coolant nanofluid (0.2% weight fraction)

Day 4: Al_2O_3- coolant nanofluid (0.4% weight fraction)

Day 5: Al_2O_3- coolant nanofluid (0.6% weight fraction)

Day 6: Al_2O_3- coolant nanofluid (0.8% weight fraction)

Day 7: Al_2O_3- coolant nanofluid (1.0% weight fraction)

4.2 Phase 1: Exp. data, sonication time and stability analysis with nanofluid

In first phase the experiments were done for two different volume fractions (0.002%, and 0.004%) of TiO_2 nanoparticles in TiO_2-Water nanofluid and Al_2O_3 nanoparticles in Al_2O_3-Water nanofluid.

The experiment was done to determine sonication time and thermal conductivity for stability analysis. The performance characteristic curves follow a nonlinear trend for all concentrations. Data collected for nano-fluid is given in the form of performance curves given with them.

4.2.1 Experiment with TiO2 nanoparticles

The sonication time for TiO_2 was determined experimentally and graph was plotted as shown below. The letters have their usual meanings given in the nomenclature of the report. The thermal conductivity increased for 80 minutes and then showed a steep decline. This means

that we have passed the optimum sonication duration. The experiment was repeated on two concentrations and in both cases it was found out to be 80 minutes.

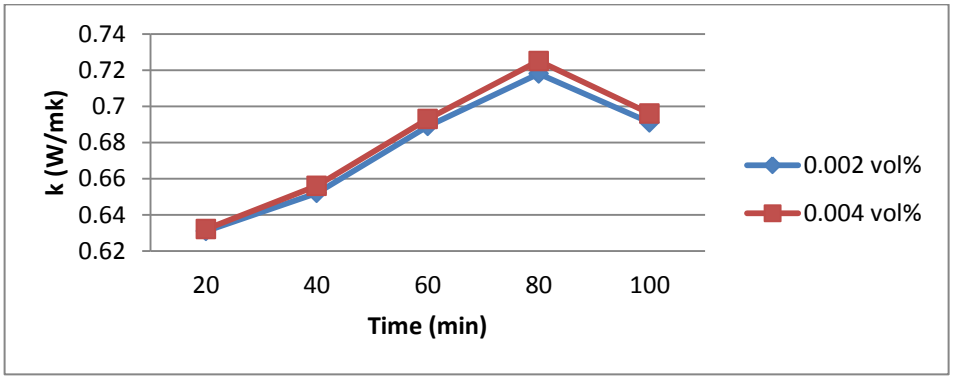

Figure 22 Sonication graph for TiO_2

4.2.2 Experiment with Al_2O_3 nanoparticles

Experiment similar to above mentioned was performed with alumina nanoparticles and sonication time was determined by standard procedure. The sonication time was found out to be 270 minutes (4 hr 30 min). The exact same data is produced when another concentration was tested.

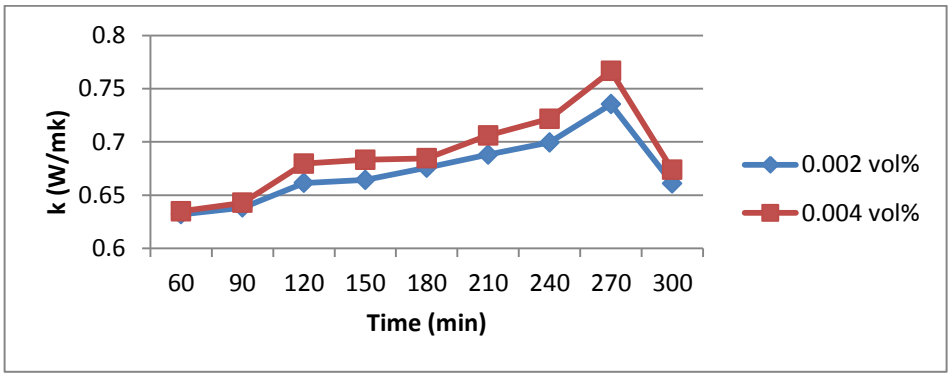

Figure 23 Sonication time for Al_2O_3

Both on papers and in the experiment Al_2O_3 nanoparticles show better properties. Table 6 and 7 can be referred in case of doubt. So aluminum oxide was chosen for further investigation.

The stability test was conducted only on Al_2O_3 nanoparticles. The test included storing the nanofluid in still container. The measurement of thermal conductivity with the help of KD2 pro was done at regular intervals. The complete procedure is mentioned in chapter 3.

The testing duration was 24 hours with 2 hour inter-test interval.

The graph was plotted between thermal conductivity and time duration passed. The optical observation procedure was not chosen in order to have a quantitative basis of stability measurement. The stability graph for Al_2O_3 is shown below.

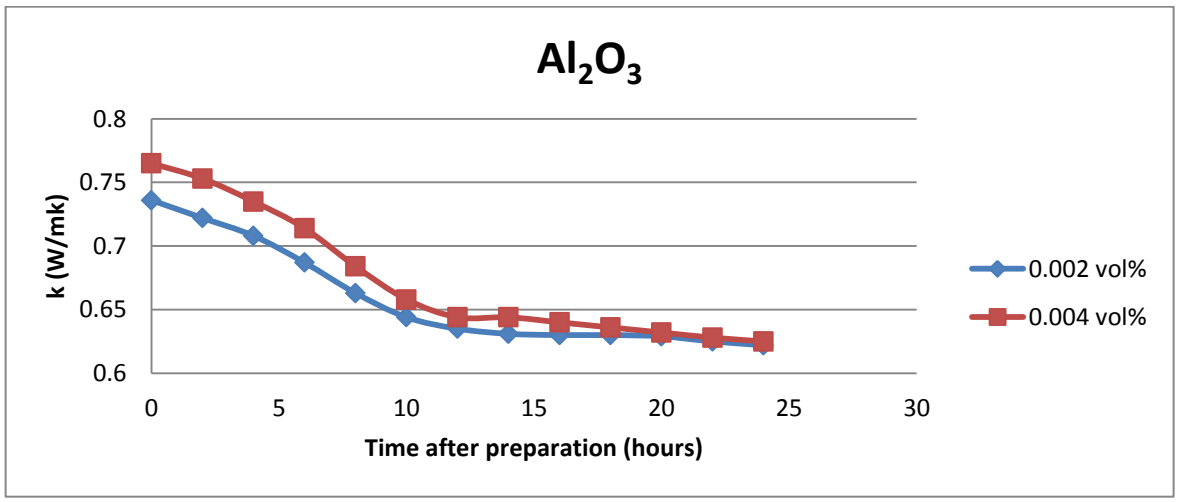

Figure 24 Stability graph for Al_2O_3

One can clearly observe that thermal conductivity first decreases very rapidly for 10 hours. Then it shows a very slow decrement in thermal conductivity and approaches to that of water at 24 hours. Most important thing to mention here is that temperature was kept constant for the duration of data recording.

The point where thermal conductivity values reached the range of 0.65 W/mK, the particle settlement was observed at the bottom of the container. So this nanofluid was stable for 10 hours as far as our purpose was concerned but that was not enough. So we have purchased the preformed nanofluid in 20 wt.% concentration stabilized with silicon oil.

This experiment when repeated with latter nanofluid showed improved stability over the previously used nanoparticles (without stabilizers).

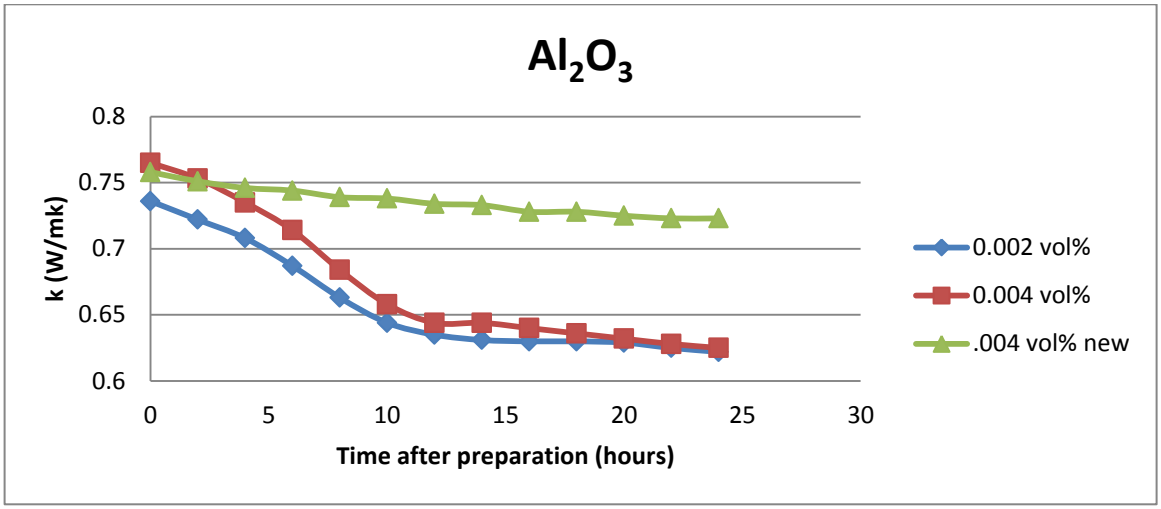

Figure 25 Stability graph for Al_2O_3 and comparision with new nanofluid

The 0.004 vol% concentration nanofluid when compared to the previous one showed tremendous stability improvement. There was no rapid decrease in stability and no particle separation was observed at this concentration. Although the maximum thermal conductivity was little lower due to silicon oil content but this is not a big issue as mean thermal conductivity is much higher.

4.3 Phase 2: Experimental analysis on engine radiator

Phase 2 of the experiment i.e. engine experimentation was done with new nanofluid in water-EG coolant. As water-EG mixture is more viscous than only water. The radiator was allowed to undergo a constant vibration when the engine was running so the nanoparticle settling was no longer a problem as the settled particles were mixed with the mainstream coolant during the next engine run.

In second phase the experiments were done for constant flow rate with five different weight fractions (0.0 %, 0.2%, 0.4%, 0.6%, 0.8% and 1.0%) of Al_2O_3 nanoparticles in EG-Water base fluid. The experiment was done from 01 Apr 2015 to 14 Apr 2015 during day time from 10:00 AM to 3:00 PM.

4.3.1 Baseline Readings (Water-EG as coolant) at 38°C ambient temperature

Table 10 Experimental results for water-EG mixture

S No.	Load(Watt)	RPM	V	I	V x I	Fuel(Kg/hr)	T_B	EGT	T_{in}	T_{out}	H_2-H_1	m_a(kg/s)	m_c (kg/s)
1	0	1535	221	0.05	11.05	0.365	49	178	55	56	5.4	0.0073	0.2500
2	500	1514	213	1.88	400.44	0.397	49	201	56	58	5.2	0.0071	0.2466
3	1000	1511	209	3.98	831.82	0.497	52	235	58	60	5.2	0.0071	0.2461
4	1500	1505	204	6.01	1226.04	0.593	55	276	61	63	5	0.0070	0.2451
5	2000	1498	196	7.69	1507.24	0.672	56	309	63	65	5	0.0070	0.2440
6	2500	1488	193	9.57	1847.01	0.761	56	352	66	68	4.8	0.0068	0.2423
7	3000	1491	186	11.13	2070.18	0.831	58	396	69	71	4.8	0.0068	0.2428
8	3500	1477	180	12.45	2241	0.952	58	445	73	75	4.6	0.0067	0.2406

Table 11 Heat balance sheet for Water-EG coolant (all values in kW)

S.No	Input	Output	Exhaust	Coolant	Body loss	Other
1	4.26	0.01	1.02	1.04	0.45	1.74
2	4.63	0.40	1.17	2.06	0.45	0.56
3	5.79	0.83	1.41	2.06	0.57	0.92
4	6.92	1.23	1.67	2.05	0.69	1.28
5	7.84	1.51	1.90	2.04	0.73	1.66
6	8.88	1.85	2.16	2.03	0.73	2.12
7	9.69	2.07	2.46	2.03	0.82	2.31
8	11.10	2.24	2.74	2.01	0.82	3.30

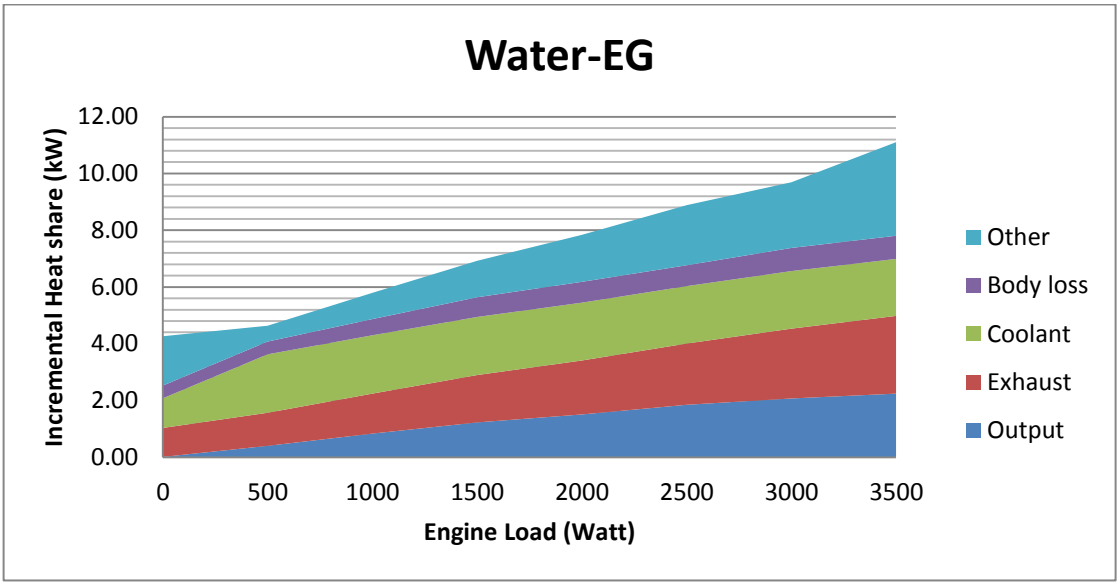

Figure 26 Variation of heat share with load for Water-EG

4.3.2 0.2 wt.% Al_2O_3 in Water–EG mixture at 41°C ambient temperature

Table 12 Experimental results for 0.2 wt.% Al_2O_3 in Water–EG mixture

S No.	Load(Watt)	RPM	V	I	V x I	FUEL(KG/ hr)	T_B	EGT	T_{in}	T_{out}	H_2-H_1	m_a(kg/s)	m_c (kg/s)
1	0	1533	217	0.05	10.85	0.368	50	218	54	56	5.4	0.0073	0.2497
2	500	1515	210	1.86	390.6	0.397	52	233	56	58	5.2	0.0071	0.2467
3	1000	1510	205	3.91	801.55	0.491	52	268	58	60	5.2	0.0071	0.2459
4	1500	1505	200	5.7	1140	0.578	55	309	61	63	5	0.0070	0.2451
5	2000	1490	194	7.62	1478.28	0.672	56	350	63	65	5	0.0070	0.2427
6	2500	1488	190	9.5	1805	0.774	56	405	66	68	5	0.0070	0.2423
7	3000	1493	186	11.1	2064.6	0.801	57	432	68	70	4.8	0.0068	0.2432
8	3500	1481	181	12.5	2262.5	0.932	58	465	71	73	4.6	0.0067	0.2412

Table 13 Heat balance sheet for 0.2 wt.% Al_2O_3 in Water–EG mixture (all values in kW)

S.No	Input	Output	Exhaust	Coolant	Body loss	Other
1	4.30	0.01	1.29	2.09	0.37	0.54
2	4.63	0.39	1.37	2.06	0.45	0.36
3	5.73	0.80	1.62	2.05	0.45	0.80
4	6.75	1.14	1.88	2.05	0.57	1.11
5	7.84	1.48	2.17	2.03	0.61	1.55
6	9.03	1.81	2.55	2.03	0.61	2.04
7	9.35	2.06	2.69	2.03	0.65	1.91
8	10.88	2.26	2.85	2.02	0.69	3.05

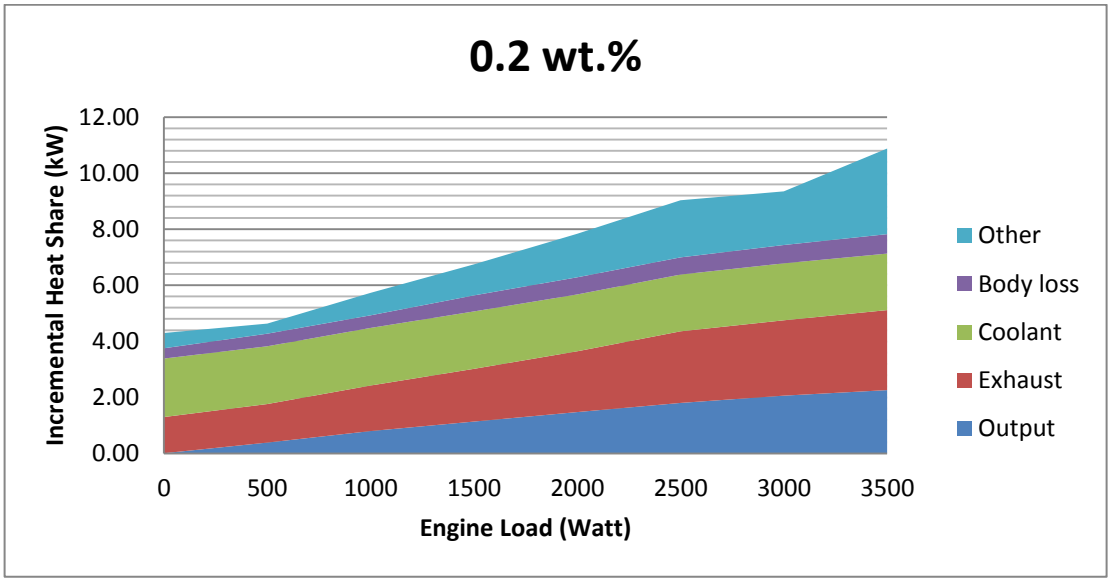

Figure 27 Variation of heat share with load for 0.2 wt.% Al_2O_3 in Water–EG mixture

4.3.3 0.4 wt.% Al_2O_3 in Water–EG mixture at 37°C ambient temperature

Table 14 Experimental results for 0.4 wt.% Al2O3 in Water–EG mixture

S No.	Load(Watt)	RPM	V	I	V x I	FUEL(KG/hr)	T_B	EGT	T_{in}	T_{out}	H_2-H_1	m_a(kg/s)	m_c(kg/s)
1	0	1530	218	0.05	10.9	0.365	49	206	54	56	5.4	0.0073	0.2492
2	500	1511	209	1.86	388.74	0.401	50	260	56	58	5.4	0.0073	0.2461
3	1000	1509	205	3.94	807.7	0.486	52	286	58	60	5.2	0.0071	0.2458
4	1500	1505	201	5.97	1199.97	0.586	55	305	60	62	5	0.0070	0.2451
5	2000	1499	198	7.71	1526.58	0.672	56	340	62	65	5	0.0070	0.2441
6	2500	1487	191	9.53	1820.23	0.761	56	388	65	67	4.8	0.0068	0.2422
7	3000	1491	186	11.12	2068.32	0.801	57	421	68	70	4.8	0.0068	0.2428
8	3500	1477	180	12.46	2242.8	0.952	57	453	71	73	4.6	0.0067	0.2406

Table 15 Heat balance sheet for 0.4 wt.% Al2O3 in Water–EG mixture (all values in kW)

S.No	Input	Output	Exhaust	Coolant	Body loss	Other
1	4.26	0.01	1.23	2.08	0.49	0.45
2	4.68	0.39	1.63	2.06	0.53	0.07
3	5.67	0.81	1.78	2.05	0.61	0.42
4	6.83	1.20	1.88	2.05	0.73	0.97
5	7.84	1.53	2.13	3.06	0.78	0.35
6	8.88	1.82	2.41	2.02	0.78	1.85
7	9.35	2.07	2.64	2.03	0.82	1.80
8	11.10	2.24	2.80	2.01	0.82	3.24

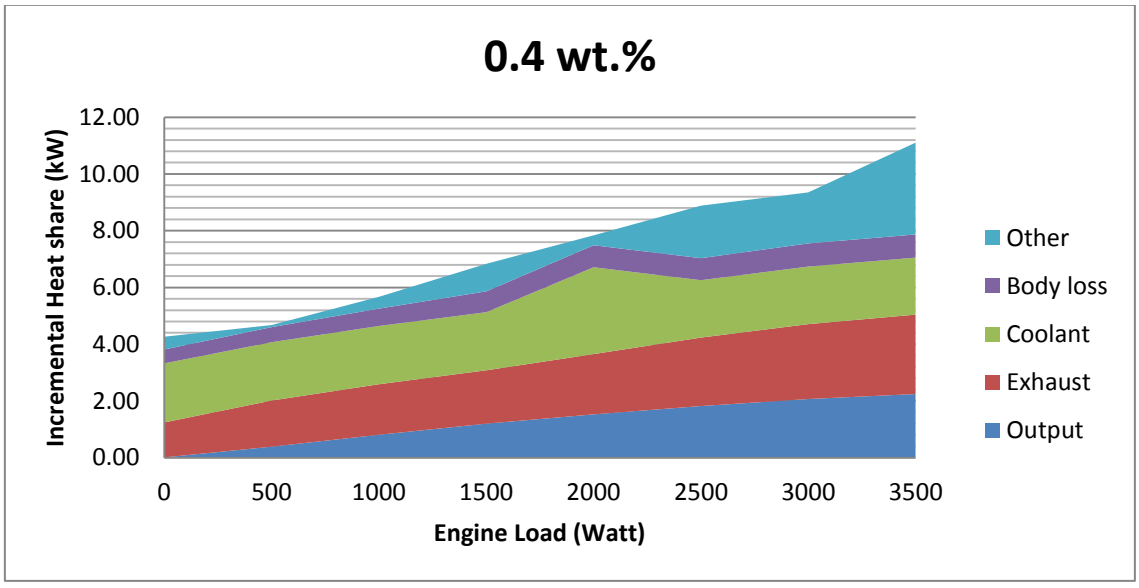

Figure 28 Variation of heat share with load for 0.4 wt.% Al2O3 in Water–EG mixture

4.3.4 0.6 wt.% Al_2O_3 in Water–EG mixture at 42°C ambient temperature

Table 16 Experimental results for 0.6 wt.% Al2O3 in Water–EG mixture

S No.	Load(Watt)	RPM	V	I	V x I	FUEL(KG/hr)	T_B	EGT	T_{in}	T_{out}	H_2-H_1	m_a(kg/s)	m_c(kg/s)
1	0	1535	217	0.05	10.85	0.365	49	201	53	55	5.4	0.0073	0.2500
2	500	1516	211	1.87	394.57	0.401	50	243	55	57	5.2	0.0071	0.2469
3	1000	1511	204	3.94	803.76	0.481	52	296	57	59	5.2	0.0071	0.2461
4	1500	1507	201	5.95	1195.95	0.593	53	319	59	62	5	0.0070	0.2454
5	2000	1496	195	7.61	1483.95	0.662	53	355	62	65	5	0.0070	0.2436
6	2500	1488	190	9.52	1808.8	0.761	55	401	65	67	4.8	0.0068	0.2423
7	3000	1493	184	11.08	2038.72	0.788	56	443	66	68	4.8	0.0068	0.2432
8	3500	1478	178	12.42	2210.76	0.952	56	465	69	72	4.6	0.0067	0.2407

Table 17 Heat balance sheet for 0.6 wt.% Al2O3 in Water–EG mixture (all values in kW)

S.No	Input	Output	Exhaust	Coolant	Body loss	Other
1	4.26	0.01	1.16	2.09	0.29	0.72
2	4.68	0.39	1.44	2.06	0.33	0.45
3	5.61	0.80	1.82	2.06	0.41	0.52
4	6.92	1.20	1.94	3.08	0.45	0.26
5	7.72	1.48	2.20	3.05	0.45	0.54
6	8.88	1.81	2.47	2.03	0.53	2.05
7	9.19	2.04	2.76	2.03	0.57	1.79
8	11.10	2.21	2.85	3.02	0.57	2.46

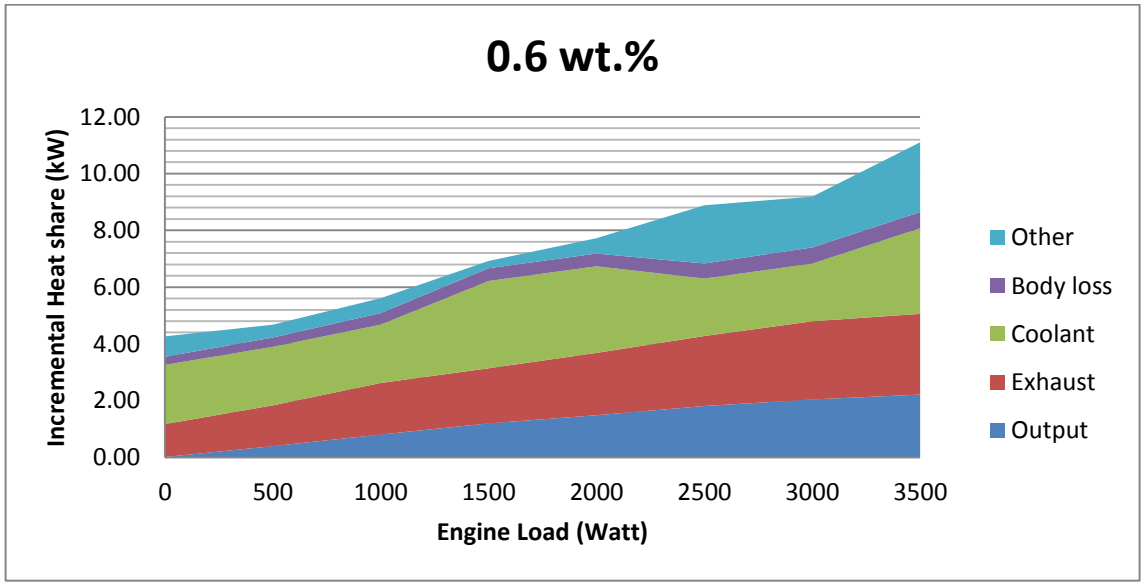

Figure 29 Variation of heat share with load for 0.6 wt.% Al2O3 in Water–EG mixture

4.3.5 0.8 wt.% Al_2O_3 in Water–EG mixture at 42°C ambient temperature

Table 18 Experimental results for 0.8 wt.% Al_2O_3 in Water–EG mixture

S No.	Load(Watt)	RPM	V	I	V x I	FUEL(KG/hr)	T_B	EGT	T_{in}	T_{out}	H_2-H_1	m_a(kg/s)	m_c(kg/s)
1	0	1532	214	0.05	10.7	0.365	49	190	52	54	5.4	0.0073	0.2495
2	500	1515	207	1.85	382.95	0.397	49	229	54	56	5.2	0.0071	0.2467
3	1000	1510	202	3.85	777.7	0.481	52	293	57	59	5.2	0.0071	0.2459
4	1500	1505	199	5.86	1166.14	0.586	54	311	59	62	5	0.0070	0.2451
5	2000	1498	194	7.59	1472.46	0.682	55	343	60	63	5	0.0070	0.2440
6	2500	1489	189	9.48	1791.72	0.774	55	391	63	66	4.8	0.0068	0.2425
7	3000	1492	184	11.04	2031.36	0.816	56	430	65	68	4.8	0.0068	0.2430
8	3500	1479	177	12.4	2194.8	0.972	56	471	67	71	4.6	0.0067	0.2409

Table 19 Heat balance sheet for 0.8 wt.% Al_2O_3 in Water–EG mixture (all values in kW)

S.No	Input	Output	Exhaust	Coolant	Body loss	Other
1	4.26	0.01	1.08	2.08	0.29	0.80
2	4.63	0.38	1.34	2.06	0.29	0.57
3	5.61	0.78	1.80	2.05	0.41	0.57
4	6.83	1.17	1.89	3.07	0.49	0.22
5	7.95	1.47	2.11	3.06	0.53	0.78
6	9.03	1.79	2.40	3.04	0.53	1.27
7	9.52	2.03	2.67	3.05	0.57	1.20
8	11.34	2.19	2.89	4.03	0.57	1.66

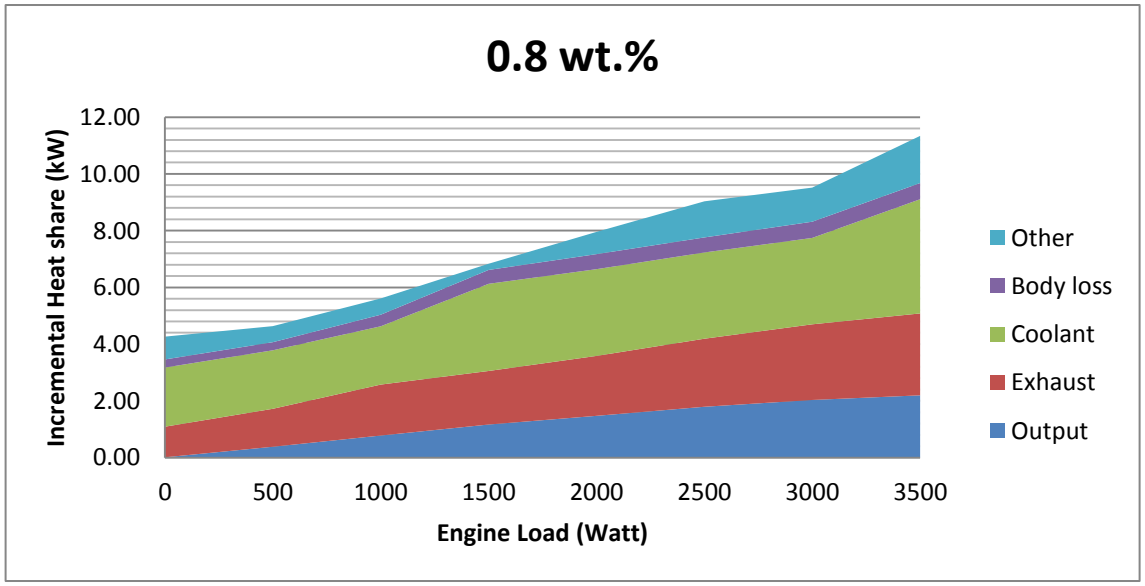

Figure 30 Variation of heat share with load for 0.8 wt.% Al_2O_3 in Water–EG mixture

4.3.6 1.0 wt.% Al_2O_3 in Water–EG mixture at 38°C ambient temperature

Table 20 Experimental results for 1.0 wt.% Al_2O_3 in Water–EG mixture

S No.	Load(Watt)	RPM	V	I	V x I	FUEL(KG/hr)	T_B	EGT	T_{in}	T_{out}	H_2-H_1	m_a(kg/s)	m_c(kg/s)
1	0	1532	215	0.05	10.75	0.365	47	203	51	53	5.4	0.0073	0.2495
2	500	1514	210	1.86	390.6	0.401	49	234	53	55	5.2	0.0071	0.2466
3	1000	1510	204	3.93	801.72	0.537	50	294	54	57	5	0.0070	0.2459
4	1500	1507	201	5.95	1195.95	0.601	51	326	56	59	5	0.0070	0.2454
5	2000	1499	196	7.64	1497.44	0.672	53	358	58	61	4.8	0.0068	0.2441
6	2500	1486	191	9.5	1814.5	0.749	53	405	60	63	4.8	0.0068	0.2420
7	3000	1491	186	11.1	2064.6	0.801	55	433	61	64	4.8	0.0068	0.2428
8	3500	1480	181	12.47	2257.07	0.952	55	465	64	68	4.6	0.0067	0.2410

Table 21 Heat balance sheet for 1.0 wt.% Al_2O_3 in Water–EG mixture (all values in kW)

S.No	Input	Output	Exhaust	Coolant	Body loss	Other
1	4.26	0.01	1.20	2.08	0.37	0.60
2	4.68	0.39	1.40	2.06	0.45	0.37
3	6.27	0.80	1.80	3.08	0.49	0.10
4	7.01	1.20	2.02	3.08	0.53	0.19
5	7.84	1.50	2.20	3.06	0.61	0.47
6	8.74	1.81	2.52	3.03	0.61	0.75
7	9.35	2.06	2.72	3.04	0.69	0.83
8	11.10	2.26	2.87	4.03	0.69	1.25

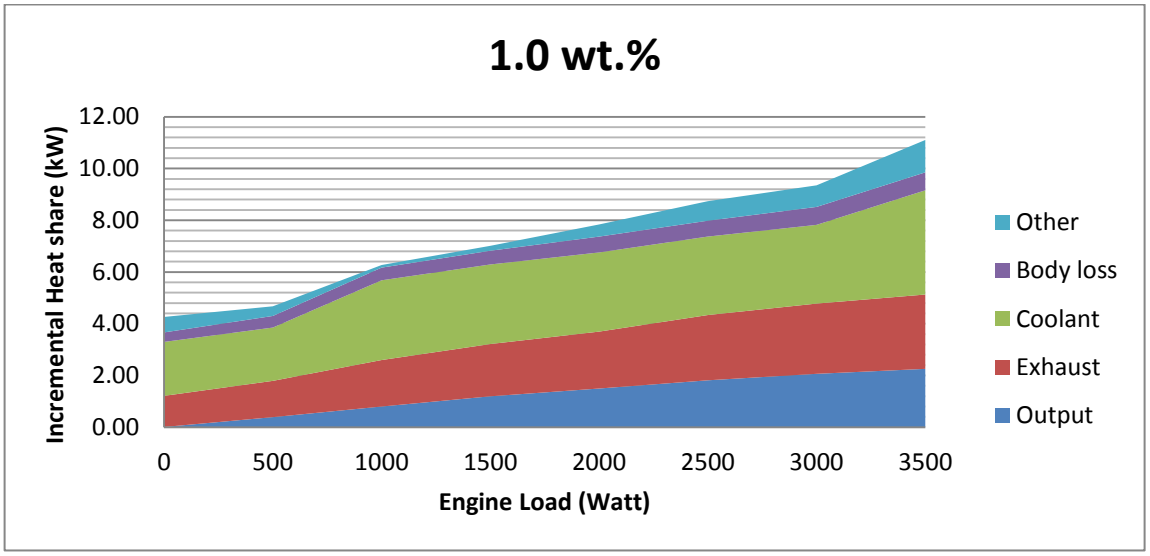

Figure 31 Variation of heat share with load for 1.0 wt.% Al_2O_3 in Water–EG mixture

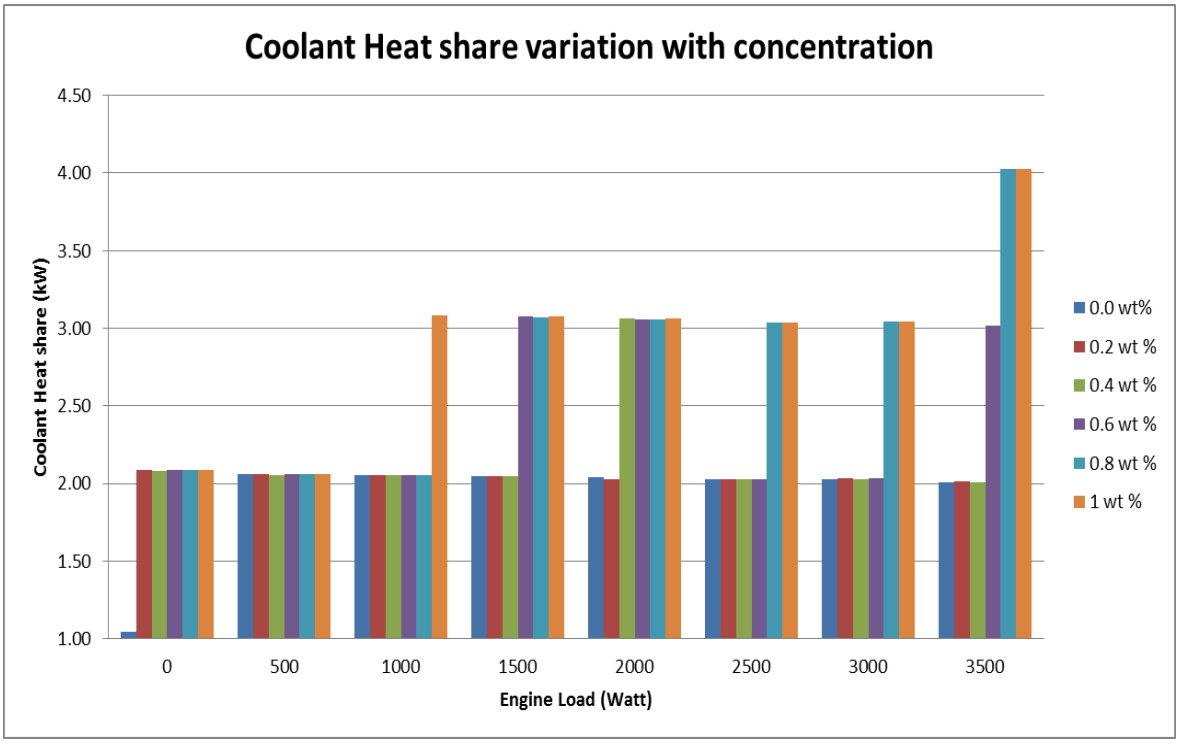

Table 22: Frontal Area reduction with each concentration

Particle Concentration (wf. %)	H_c (avg.) kW	Ratio(H_c/baseline)	Area required for baseline heat transfer	% Area reduction
Baseline (0.0)	1.91	1.00	1.00	0.00
0.2	2.04	1.07	0.94	6.37
0.4	2.17	1.14	0.88	11.98
0.6	2.43	1.27	0.79	21.40
0.8	2.81	1.47	0.68	32.03
1.0	2.93	1.53	0.65	34.81

4.4 Result Analysis

The performance of Radiator was analyzed with water/Ethylene Glycol and Al_2O_3 nano-fluid of 0.0%, 0.2%, 0.4%, 0.6%, 0.8% and 1.0% weight percent under various conditions. The analysis was done on eight different load conditions i.e. no load , 500 W, 1000 W, 1500 W, 2000 W, 2500 W, 3000 W and 3500 W for both water/EG and nano-fluid. Analysis of the results and data is presented here.

The most important parameter is the heat share curve. The vertical axis refers to the incremental heat rate at a particular time i.e. instantaneous heat balance. The instantaneous heat balance refers to the share of input heat energy dissipated in each component on the engine (coolant, exhaust, body loss, power production etc.)at particular instant. The horizontal axis shows the load applied on the engine with the help of electric dynamometer.

The area of the graph represents their heat loss factors. The smaller the area, the less is the heat share. A line with a small slope represents that heat loss share is very less as compared to one with higher slope when load is increased.

4.4.1 Result analysis at EG-Water mixture (BASELINE)

Fig 26 describes the comparison of the performance characteristics of 0 wt.% nanofluids (i.e Water-EG mixture) at 15 lpm flow rate. The maximum thermal efficiency of 31% was achieved at 3 kW of engine load. The radiator temperature rise was normal and nearly constant with load. The coolant heat loss also remained constant at about 2 kW. Graph below represents the coolant heat loss variation with load.

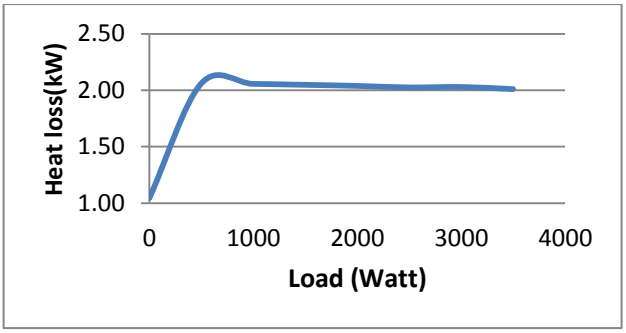

Figure 32 Coolant heat loss at 0% nanofluid concentration

4.4.2 Result analysis at .2 wt.% Al_2O_3-Water/EG mixture

Fig 27 describes the comparison of the performance characteristics of 0.2 wt.% nanofluid at 15 lpm flow rate. The performance characteristics are similar to those of 'coolant only' conditions The maximum thermal efficiency of 32% was achieved at 3 kW of engine load. The radiator temperature rise was normal and linear with load. The coolant heat loss also remained constant at about 2.09 kW and decreasing as load was increased. Graph below represents the coolant heat loss variation with load.

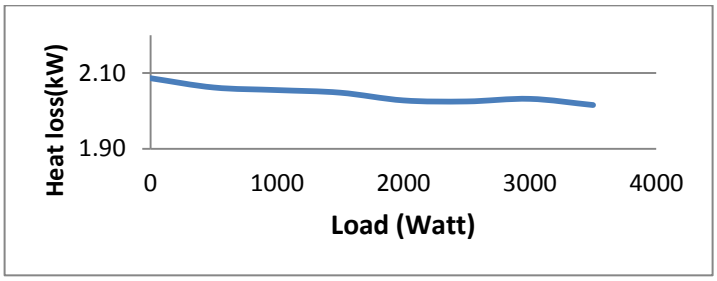

Figure 33 Coolant heat loss at 0.2 wt.% nanofluid concentration

4.4.3 Result analysis at .4 wt.% Al_2O_3-Water/EG mixture

Fig 28 describes the comparison of the performance characteristics of 0.4 wt.% nanofluid at 15 lpm flow rate. The performance characteristics showed a deviation when compared to baseline conditions The maximum thermal efficiency of 32% was achieved at 3 kW of engine load. The radiator temperature rise was normal and linear with load. The coolant heat loss remained constant at about 2 kW till 1500 watt then showed a peak of 3 kW at 2000 watt load. The load then decreased to previous values on further loading. Graph below represents the coolant heat loss variation with load.

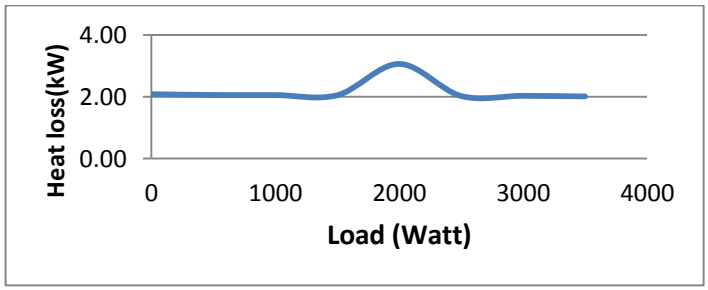

Figure 34 Coolant heat loss at 0.4 wt.% nanofluid concentration

4.4.4 Result analysis at .6 wt.% Al_2O_3-Water/EG mixture

Fig 29 describes the comparison of the performance characteristics of 0.6 wt.% nanofluid at 15 lpm flow rate. Like previous concentration the performance characteristic showed a deviation when compared to baseline conditions The maximum thermal efficiency of 33% was achieved at 3 kW of engine load. The radiator temperature rise was normal and linear with load. The coolant heat loss varied constantly and showed a peak of 3.08 kW at 2000 watt load. The load then decreased and then increased on further loading. The increased thermal conductivity of the coolant started showing its effects on the cooling performance. The heat share of coolant is significantly increased. Graph below represents the coolant heat loss variation with load.

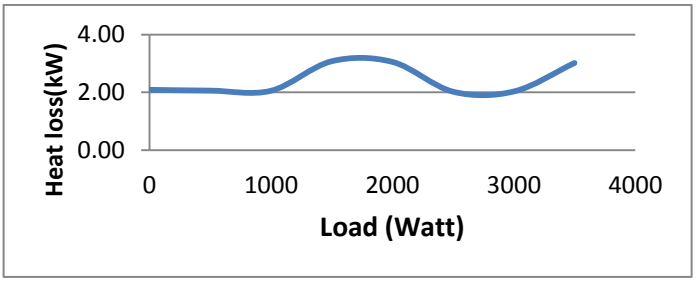

Figure 35 Coolant heat loss at 0.6 wt.% nanofluid concentration

4.4.5 Result analysis at .8 wt.% Al_2O_3-Water/EG mixture

Fig 30 describes the comparison of the performance characteristics of 0.8 wt.% nanofluid at 15 lpm flow rate. The performance characteristics show a greater deviation when compared to baseline conditions The maximum thermal efficiency of 32% was achieved at 3 kW of engine load. The radiator temperature rise was increasing non linearly with load. The coolant heat loss showed a constantly increasing trend with increase in load and is maximum at maximum rated engine load and the numerical value is 4.03 kW, the increased heat dissipation by coolant started at low load of 1500 Watt.. The increased thermal conductivity of the coolant started showing its effects on the cooling performance. The heat share of coolant is significantly increased especially at higher loads. Graph below represents the coolant heat loss variation with load.

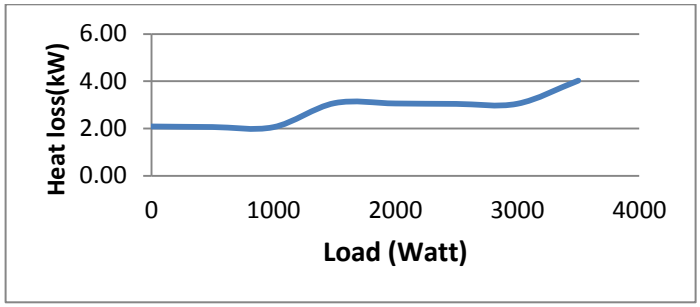

Figure 36 Coolant heat loss at 0.8 wt.% nanofluid concentration

4.4.6 Result analysis at 1.0 wt.% Al_2O_3-Water/EG mixture

Fig 31 describes the comparison of the performance characteristics of 1.0 wt.% nanofluid at 15 lpm flow rate. The performance characteristic shows a deviation when compared to baseline conditions The maximum thermal efficiency of 32% was achieved at 3 kW of engine load. The radiator temperature rise was increasing non linearly with load. The coolant heat loss showed a constantly increasing trend with increase in load and is maximum at maximum rated engine load and the numerical value is 4.03 kW. The increased heat dissipation by coolant started at low load of 1000 Watt. The increased thermal conductivity of the coolant started showing its effects on the cooling performance. The heat share of coolant is significantly increased especially at higher loads. Graph below represents the coolant heat loss variation with load.

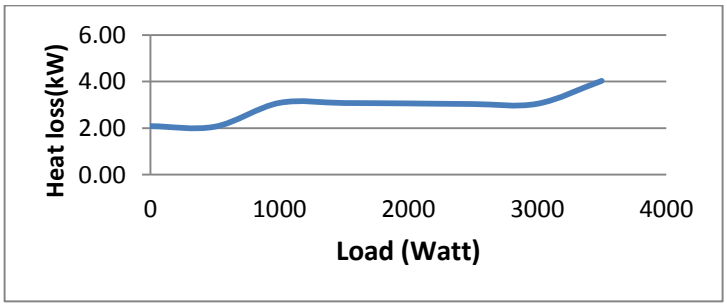

Figure 37 Coolant heat loss at 1.0 wt.% nanofluid concentration

Chapter 5 Conclusion

The two most commonly available nanofluids (TiO_2 and Al_2O_3) were tested for stability and thesis sonication time was determined experimentally. The nanofluid with superior properties was tested on water cooling system for single cylinder diesel engine which was fabricated and assembled. Detailed experimental study has been carried out in various outdoor conditions and at different mass fraction concentrations of nanoparticles i.e. 0.0%, 0.2%, 0.4%, 0.6%, 0.8% and 1.0% w.f.

Firstly stability analysis of nanofluid was conducted at ambient conditions two different concentrations of nanofluid for both nanoparticles and it was observed that the higher stability was shown by the aluminum oxide nanofluid sample under all the conditions. It was observed that at lower volume fraction the particle agglomeration of nanofluid is less in first few hours of nanofluid preparation, higher concentration showed greater deterioration in thermal conductivity. The thermal conductivity approached to that of water at 24 hours of preparation hence the nanofluid was considered unsuitable for engine experimentation.

The preformed and stabilized aluminum oxide nanofluid was purchased from a vender in 20 wt.% concentration. The required concentration was made by mixing different volumes of this nanofluid. 0.004 vol% concentration was tested for stability and compared with the previous readings. The stability increment was many folds and the fluid became suitable for engine experimentation.

The vibrational aspects of the engine moving parts were utilized in keeping the coolant-nanofluid mixture in agitated state inside the radiator during the experiment, so particle settlement became least of the worries. Also the particle settlement from previous experiment was mixed with mainstream coolant due to engine vibrations and high coolant flow rate. Hence incremental mixing process was adopted in same coolant mixture when concentration was increased.

At baseline conditions the thermal efficiency of 31% is achieved at 3 kW engine load. The average coolant heat loss was 1.91 kW at these loading conditions. The ambient

temperature being 38°C, there was a considerable portion of heat going waste into the atmosphere.

On 0.2 wt.% nanoparticle concentration the heat balance showed similar results as were with baseline readings so low nanoparticle concentration seems to have negligible effect on thermal performance of the engine. The average coolant heat loss was 2.04 kW. A higher thermal efficiency of 32% was achieved which was mainly due to higher ambient temperature where average heat loss was less as compared to baseline. On further increasing the nanoparticle concentration the coolant heat share increased. The increased thermal conductivity of coolant medium started showing its effect. The thermal efficiency of the engine remained same as in the previous case.

At 0.6wt.% nanoparticle concentration the heat loss in the radiator becomes even more. The average of 2.45 kW coolant heat loss was obtained at this concentration. The ambient temperature was 42°C and remained constant throughout the experiment. The maximum thermal efficiency achieved was 33% which is highest among all the experimental readings.

On increment in nanoparticle concentration the average heat loss over all loads was 2.81 kW and 2.93 kW for 0.8 wt.% and 1.0 wt.% respectively. For higher nanoparticle concentration heat rejection was higher which enhanced the thermal performance of the radiator and also the nanoparticles agglomeration problem started to appear at 1 wt.%, the particle settlement was of temporary nature and remixing takes place during next engine run.

The maximum 34.81% area reduction was achieved at 1 wt.% concentration as compared to the baseline conditions. The area reduction was found out to be significant as it may help in reducing vehicle's frontal area and hence the drag. This will be an added advantage along with weight and space savings. Also the reduced area means use of smaller radiator for same heat transfer hence reducing the initial equipment cost.

5.1 Scope for future work

As very little work has been done on engine radiator with nanofluid based coolant so far, therefore a lot of work is still to be done. Some recommendations for the future work are as follows:

- Comparative study on different types of radiators can be done by using different base fluids and same nanoparticles or same base fluid with different nanoparticles.
- The effect of flow rate can be checked by using variable flow rate.
- The effect of inclination angle of the radiator should be studied.
- The effect of radiator dimensions on the performance can be analyzed.
- The performance can be analyzed using multiple pass arrangement.
- The performance can be analyzed by changing gap between radiator tubes and fins.
- The effect of wind velocity on the performance can be analyzed.
- Surfactants can be used to improve the stability of the nanofluids.
- Higher concentrations of nanofluids may be tested.

References

[1] Y Xuan, Q Li, "Heat transfer enhancement of nanofluids" International Journal of Heat and fluid flow 21 (2000) 58–64.

[2] P. Keblinski, S.R. Phillpot, S.U.S. Choi, J.A. Eastman, "Mechanisms of heat flow in suspensions of nano-sized particles (nanofluids)", International Journal of Heat and mass transfer 45 (2002) 855–863.

[3] X-Qi. Wang, A.S. Mujumdar, "Heat transfer characteristics of nanofluids: a review", International Journal of Thermal Sciences 46 (2007) 1–19.

[4] H. A. Mintsa, G Roy , C. T Nguyen, D Doucet, "New temperature dependent thermal conductivity data for water-based nanofluids", International Journal of Thermal Sciences 48 (2009) 363–371.

[5] W Duangthongsuk, S Wongwises, "Measurement of temperature-dependent thermal conductivity and viscosity of TiO2-water nanofluids", Experimental Thermal and Fluid Science 33 (2009) 706–714.

[6] H. Chena, S Witharana, Yi Jin, C. Kim, Y. Ding, "Predicting thermal conductivity of liquid suspensions of nanoparticles (nanofluids) based on rheology", Particuology 7 (2009) 151–157.

[7] D Wen, G Lin, S Vafaei, K. Zhang, "Review of nanofluids for heat transfer applications", Particuology 7 (2009) 141–150

[8] L. S. Sundar, M. K. Singh, A. C.M. Sousa, "Investigation of thermal conductivity and viscosity of Fe_3O_4 nanofluid for heat transfer applications", International Communications in Heat and Mass Transfer 44 (2013) 7–14.

[9] L. S. Sundar, Md. H. Farooky, S. N. Sarada, M.K. Singh, "Experimental thermal conductivity of ethylene glycol and water mixture based low volume concentration of Al2O3 and CuO nanofluids", International Communications in Heat and Mass Transfer 41 (2013) 41–46

[10] R. S. Khedkar, S.S. Sonawane, K. L. Wasewar, "Heat transfer study on concentric tube heat exchanger using TiO2–water based nanofluid", International Communications in Heat and Mass Transfer 57 (2014) 163–169.

[11] H. Maddah, M Alizadeh, N Ghasemi, S Rafidah, W. Alwi, "Experimental study of Al2O3/water nanofluid turbulent heat transfer enhancement in the horizontal double pipes fitted with modified twisted tapes", International Journal of Heat and Mass Transfer 78 (2014) 1042–1054.

[12] Ji Zhang, Y. Diao, Y. Zhao, Y. Zhang, "Experimental study of TiO2–water nanofluid flow and heat transfer characteristics in a multiport mini-channel flat tube", International Journal of Heat and Mass Transfer 79 (2014) 628–638.

[13] M Sheikholeslami, D.D. Ganji, "Nanofluid flow and heat transfer between parallel plates considering Brownian motion using DTM", Comput. Methods Appl. Mech. Engg. 283 (2015) 651–663.

[14] M.C.S. Reddy, V.V. Rao, "Experimental investigation of heat transfer coefficient and friction factor of ethylene glycol water based TiO2 nanofluid in double pipe heat exchanger with and without helical coil inserts", International Communications in Heat and Mass Transfer 50 (2014) 68–76.

[15] S.S. Sonawane, Rohit S. Khedkar, Kailas L. Wasewar, "Effect of sonication time on enhancement of effective thermal conductivity of nano TiO2–water, ethylene glycol, and paraffin oil nanofluids and models comparisons", Journal of Experimental Nanoscience, 2013.

[16] D.P. Kulkarni, R.S. Vajjha, D.K. Das, D. Oliva, "Application of aluminum oxide nanofluids in diesel electric generator as jacket water coolant", Applied Thermal Engineering 28 (2008) 1774–1781.

[17] K.Y. Leong, R. Saidur, S.N. Kazi, A.H. Mamun, "Performance investigation of an automotive car radiator operated with nanofluid-based coolants (nanofluid as a coolant in a radiator)", Applied Thermal Engineering 30 (2010) 2685-2692.

[18] S.M. Peyghambarzadeh, S.H. Hashemabadi, S.M. Hoseini, M. Seifi Jamnani, "Experimental study of heat transfer enhancement using water/ethylene glycol based nanofluids as a new coolant for car radiators", International Communications in Heat and Mass Transfer 38 (2011) 1283–1290.

[19] A.M. Hussein, R.A. Bakar, K. Kadirgama, K.V. Sharma, "Heat transfer enhancement using nanofluids in an automotive cooling system", International Communications in Heat and Mass Transfer 53 (2014) 195–202.

[20] O.Mahian , A. Kianifar , S.A. Kalogirou , I. Pop, S. Wongwises, "A review of the applications of nanofluids in solar energy", International Journal of Heat and Mass Transfer 57 (2013) 582–594.

[21] A. Ghadimi, I.H. Metselaar, "The influence of surfactant and ultrasonic processing on improvement of stability, thermal conductivity and viscosity of titania nanofluid." Experimental Thermal and Fluid Science 51 (2013) 1–9.

[22] M.Ghanbarpour, E.Bitaraf, R.Khodabandeh,"Thermal properties and rheological behaviour of water based al2o3 nanofluid as a heat transfer fluid", Experimental Thermal and Fluid Science 53 (2014) 227–235.

[23] D.H. Yoo, K. S. Hong and T. E. Hong, J. A. Eastman, H.S. Yang," Thermal Conductivity of Al2O3/Water Nanofluids", Journal of the Korean Physical Society, Vol. 51, October 2007, pp. S84_S87.

[24] N. A. C. Sidik, H. A. Mohammed, O. A. Alawi, S. Samion, "A review on preparation methods and challenges of nanofluids", International communication in Heat and Mass Transfer 54 (2014) 115-125.

[25] X.F. Li , D.S. Zhu, X.J. Wang , N. Wang, J.W. Gao, H. Li, "Thermal conductivity enhancement dependent pH and chemical surfactant for Cu-H2O nanofluids", Thermochimica Acta 469 (2008) 98–103.

[26] G. Xia, H. Jiang, R. Liu, Y. Zhai, Effects of surfactant on the stability and thermal conductivity Al2O3/de-ionized water nanofluids.

Appendix 1 : List of consumables

S. No.	Items/Materials	Quantity
1.	Radiator stand	1
2.	Coolant Circulation pump	1
3.	Fan and fan belt assembly	1
4.	Adhesives	-
5.	Thermocouples	4
6.	Connecting hoses with clips	3
7.	Fixing bolts	10+
8.	Coupling with pulley	1
9.	Labour charges(Welding etc)	
10.	Aluminum oxide Nanofluid	500ml
11.	Diesel fuel	30 liter
12.	Nipple 3inch	2
13.	25 mm T	1
14.	25mm stopper	1
15.	G.I. pipe 1.5“	1
16.	Pump valve 25 mm	1
17.	Exhaust manifold socket	1
18.	Engine coolant	3 Litre
19.	D-I water	25 Litre

Appendix 2: Nanofluid datasheet

S.No	Property	Value
1.	Vendor	Nanoshel (Intelligent Materials Pvt. Ltd.)
2.	Name	Aluminium Oxide (Al_2O3 Alpha) Nano powder dispersion in Water
3.	Appearance	Milky Liquid
4.	pH value	2 to 5
5.	Original Particle Size	30 nm
6.	Crystal Structure and Type	Alpha
7.	Concentration	20 wt. %
8.	Solvent	water 80%
9.	Surface treating compound	Silicon oil (1 wt. %)
10.	Fe (Iron)	$\leq$ 3 ppm
11.	Arsenic	$\leq$ 2 ppm
12.	Pb (lead)	$\leq$ 10 ppm
13.	Purity	99.99%